evaluated if increased *Tgfb1* expression reflected intracellular signal transduction (Fig. 3*B*). As a positive control, exogenously applied TGF-β1 potently induced the C-terminal phosphorylation of Smad2, which was weakened by SB431542. Importantly, in BMP-2-treated ATDC5 chondrocytes, Smad2 was phosphorylated at a comparatively weak but detectable level, which was suppressed by SB431542 (Fig. 3*B*). In addition, an immunocytochemistry for phosphorylated Smad2 in ATDC5 cells showed that endogenous TGF-β signaling was activated in BMP-2-treated chondrocytes, which was blocked by SB431542 (Fig. 3*C*). These data indicated that the activation of Smad2 by BMP-2 was achieved through the TGF-β type I receptor, probably by the up-regulated production of TGF-β1 in ATDC5 cells. In developing humerus growth plate of E17.5 mouse embryo, moderate expression of TGF-β1 was detected in proliferative chondrocytes, suggesting its role in promoting early chondrogenesis (Fig. 3*D*). Importantly, the expression of TGF-β1 was further accentuated in the prehypertrophic zone and the matrix around the hypertrophic chondrocytes (Fig. 3*D*). Similarly, Smad2 was phosphorylated in some of the proliferative chondrocytes, whereas phospho-Smad2 was detected in most of the prehypertrophic chondrocytes (Fig. 3*D*). Interestingly, Smad2 was not phosphorylated in hypertrophic chondrocytes. These results from immunohistochemistry suggested that expression of TGF-β1 was elevated to up-regulate TGF-β signaling in prehypertrophic chondrocytes, whereas the signaling was inhibited with in hypertrophic chondrocytes, in the endochondral ossification process.

Because Smad3 signaling had been suggested to suppress BMP pathway in maturing chondrocytes (26), we examined immunoblotting for the phosphorylated Smad1/5/8 to investigate the role of endogenous TGF-β signaling against the BMP-Smad signaling system in chondrocytes. BMP-2 induced potent C-terminal phosphorylation of Smad1/5/8 in ATDC5 cells, even at day 4 of induction, whereas combined treatment with SB431542 showed no effect (Fig. 3*E*). However, interestingly, the expression of *Id1*, a specific direct target of the canonical BMP-Smad pathway (33), was significantly elevated by SB431542 treatment, whereas it was suppressed by exogenously applied TGF-β1 (Fig. 3*F*). These data suggest that BMP-induced activation of endogenous TGF-β signaling inhibited BMP signaling downstream of R-Smad activation as a negative feedback mechanism. These data also confirmed that SB431542 is an appropriate tool to screen for putative molecular mediator(s) downstream of endogenous TGF-β signaling to inhibit BMP signaling in chondrocytes.

SnoN Is Induced by Endogenous TGF-β Signaling in Maturing Chondrocytes—The BMP signaling system is negatively regulated at multiple steps (*e.g.* by extracellular antagonists (*e.g.* Noggin, Chordin, Dan, and Cerberus), inhibitory Smads (I-Smads; Smad6 and Smad7), E3 ubiquitin ligases (*e.g.* Smurf1 and Smurf2), and the Ski/SnoN family of transcriptional corepressors) (34, 35). We asked if any of these BMP signaling inhibitors were induced downstream of endogenous TGF-β signaling in maturing chondrocytes. In micromass cultures of ATDC5 chondrocytes, treatment with TGF-β1, as positive control, significantly elevated only the expression of *Smad7* and *SnoN*, both of which are the direct target genes of the TGF-β-Smad pathway (supplemental Fig. 1). In BMP-2-induced maturing cells, *Smad6*, *Smad7*, and *SnoN* were up-regulated, whereas combined treatment with SB431542 completely inhibited only the elevation of *SnoN* (supplemental Fig. 1). In mouse primary chondrocytes at day 14 of BMP treatment, SnoN was also significantly elevated; this effect was not observed by combined application with SB431542 (Fig. 4*A*). These data indicate that, among the examined BMP inhibitors, SnoN was exclusively induced by the enhanced endogenous TGF-β signaling in maturing chondrocytes. During the maturation phase of ATDC5 chondrocytes, the level of *SnoN* mRNA was increased from days 4 to 10 of BMP application and mildly decreased thereafter, whereas this effect was completely prevented by SB431542 (Fig. 4*B*). Because SnoN is an unstable protein, which has a half-life of 30 min in the presence of TGF-β signaling (36, 37), we asked if the protein level of SnoN reflects the pattern of its mRNA expression and performed an immunoblot for SnoN protein (Fig. 4*C*). As control to identify specific bands for endogenous SnoN protein, we performed a knockdown assay against *SnoN* in monolayer cultures of ATDC5 cells (Fig. 4*C*, *lanes 5–7*). At day 3, the signals of two major bands of around 80 kDa were increased in BMP-2-treated cells, both of which were efficiently abolished by siSnoN, indicating that these bands represented the two isoforms, SnoN and SnoN2 (38). In micromass cultures of ATDC5 chondrocytes at day 7 of BMP-2 application, SnoN protein expression was also induced and further weakened by SB431542 (Fig. 4*C*, *lanes 1–4*), indicating that the expression of the SnoN protein was indeed induced by endogenous TGF-β signaling in maturing chondrocytes. We also confirmed the induction of SnoN protein by immunocytochemistry. Treatment with TGF-β1 for 16 h potently increased the signal of SnoN protein, which was only faintly detected in cells transfected with SnoN siRNA (Fig. 4*D*). At day 4 of BMP-2 stimulation, the level of SnoN protein was up-regulated, which was weakened by siSnoN, in maturing ATDC5 chondrocytes of monolayer cultures (Fig. 4*E*). The knockdown efficiency of SnoN in BMP-2-treated cells was relatively weak, probably because 5 days had passed since the transfection of siRNA. Next, to confirm that the inhibitory effect of SB431542 against the expression level of *SnoN* was exclusive for the late maturation phase, we stimulated ATDC5 cells with BMP-2 in combination with SB431542 and harvested the cells at the early time points within 36 h of induction (Fig. 4*F*). To our surprise, *SnoN* was rapidly induced by BMP-2 after 1 h and was decreased to reach the basal level thereafter, an expression pattern that was similar to that of *Id1* (Fig. 4*F*). However, this transient induction of *SnoN* by BMP-2 was not affected by SB431542, suggesting that endogenous TGF-β signaling was not responsible for this up-regulation of *SnoN*.

To investigate the possibility that SnoN plays a role in chondrogenesis *in vivo*, its expression in cartilage tissue was examined. We extracted RNA from various tissues of 3-month-old adult mice to prepare tissue panels of cDNA to analyze the tissue distribution. Consistent with the report that heterozygous *SnoN* knock-out mice developed T lymphomas in the spleen, which indicates an important role of SnoN in the spleen (39), we detected the highest level of *SnoN* expression in the spleen (Fig. 4*G*). Interestingly, the comparatively highest level

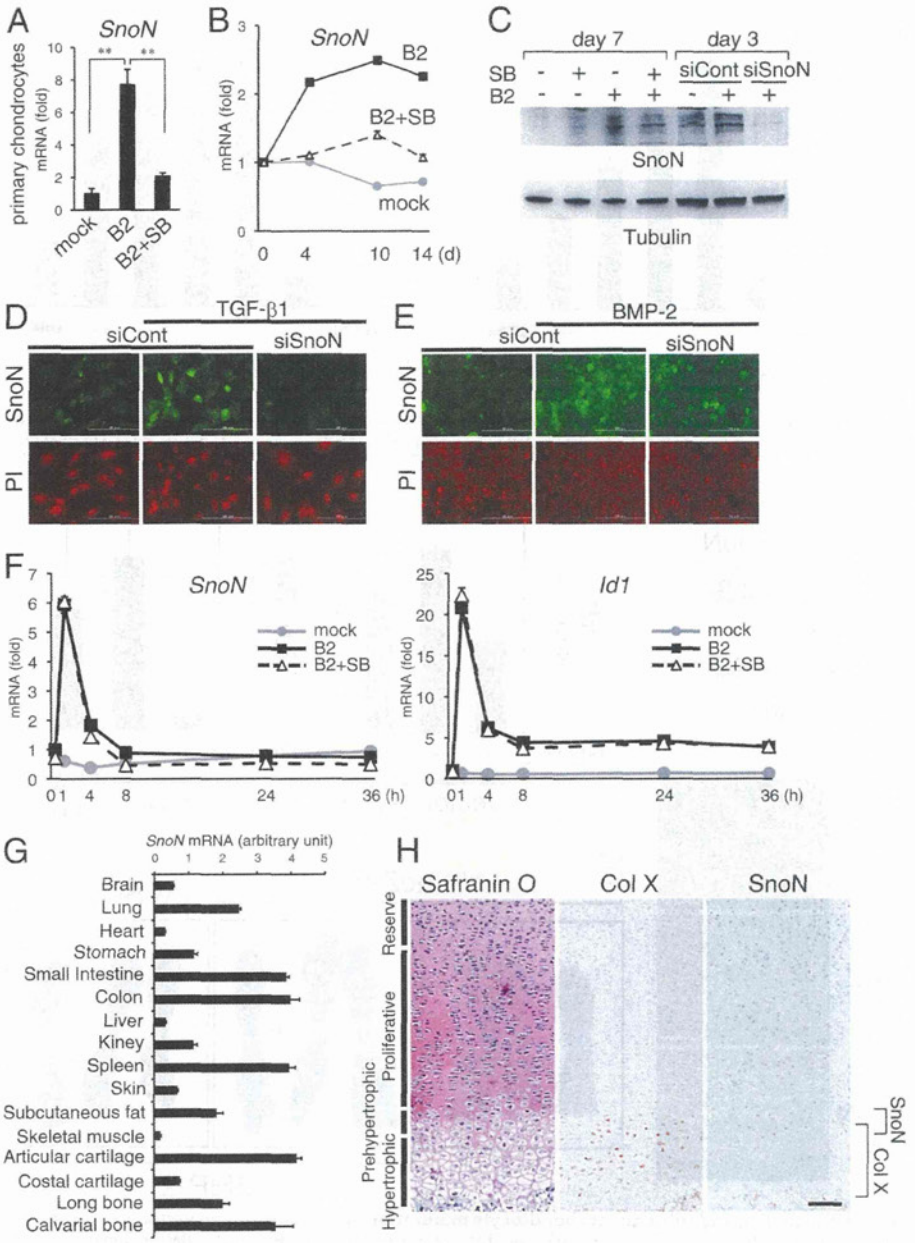

FIGURE 4. **SnoN is induced in maturing chondrocytes by endogenous TGF-β signaling *in vitro*, whereas it is highly expressed in cartilage tissue in mice.** *A*, expression of *SnoN* in primary chondrocytes at day 14 of stimulation was evaluated by real-time RT-PCR. Cells were stimulated with BMP-2 (*B2*; 300 ng/ml) with or without SB431542 (*SB*; 1 μM). *B*, ATDC5 chondrocytes were cultured with BMP-2 with or without SB431542 for the indicated times, after which the samples were subjected to qPCR analysis for *SnoN*. *C*, expression of SnoN protein in ATDC5 cells was assessed by immunoblotting. Differentiation of ATDC5 cells was induced by incubation with BMP-2 for 7 days (*lanes 1–4*). As a control, cells were transfected with siSnoN for 16 h and further cultured in the presence of BMP-2 for 3 days (*lanes 5–7*). Tubulin served as a loading control. *D* and *E*, immunocytochemistry for SnoN was performed on a monolayer culture of ATDC5 cells. Cells were transfected with siRNA for 16 h and further incubated with or without TGF-β1 (5 ng/ml) for 16 h (*D*) or with or without BMP-2 for 4 days (*E*). MG132 (10 μM) was applied 16 h prior to cell fixation. Nuclei were visualized with propidium iodide (*PI*). *Scale bars*, 100 μm. *F*, ATDC5 chondrocytes were stimulated with BMP-2 in combination with SB431542 for the indicated time points. cDNA samples were subjected to qPCR analysis for *SnoN* and *Id1*. *G*, tissue cDNA panel of 3-month-old mice was subjected to real-time PCR for *SnoN*. *H*, protein expression of type X collagen (*Col X*) and SnoN in E17.5 humerus cartilage was determined by immunohistochemistry. Zones of positive signal were indicated. Proteoglycans in cartilage matrix were stained by Safranin O. *Scale bar*, 100 μm. **, $p < 0.01$. *Error bars*, S.D.

of *SnoN* expression was found in articular cartilage (Fig. 4*G*). Immunohistochemistry for the growth plate of developing bone of mouse embryos at E17.5, in which endochondral ossification was in progress, detected the signal of type X collagen protein from the lower half of prehypertrophic chondrocytes to the entire area of hypertrophic chondrocytes (Fig. 4*H*). Importantly, although SnoN protein was detected weakly in proliferating chondrocytes, its potent signal was present in prehypertrophic chondrocytes, whereas it was weakened in hypertrophic chondrocytes (Fig. 4*H*). These data suggest that SnoN is highly expressed in premature chondrocytes before hypertrophic conversion, *in vitro* and *in vivo*.

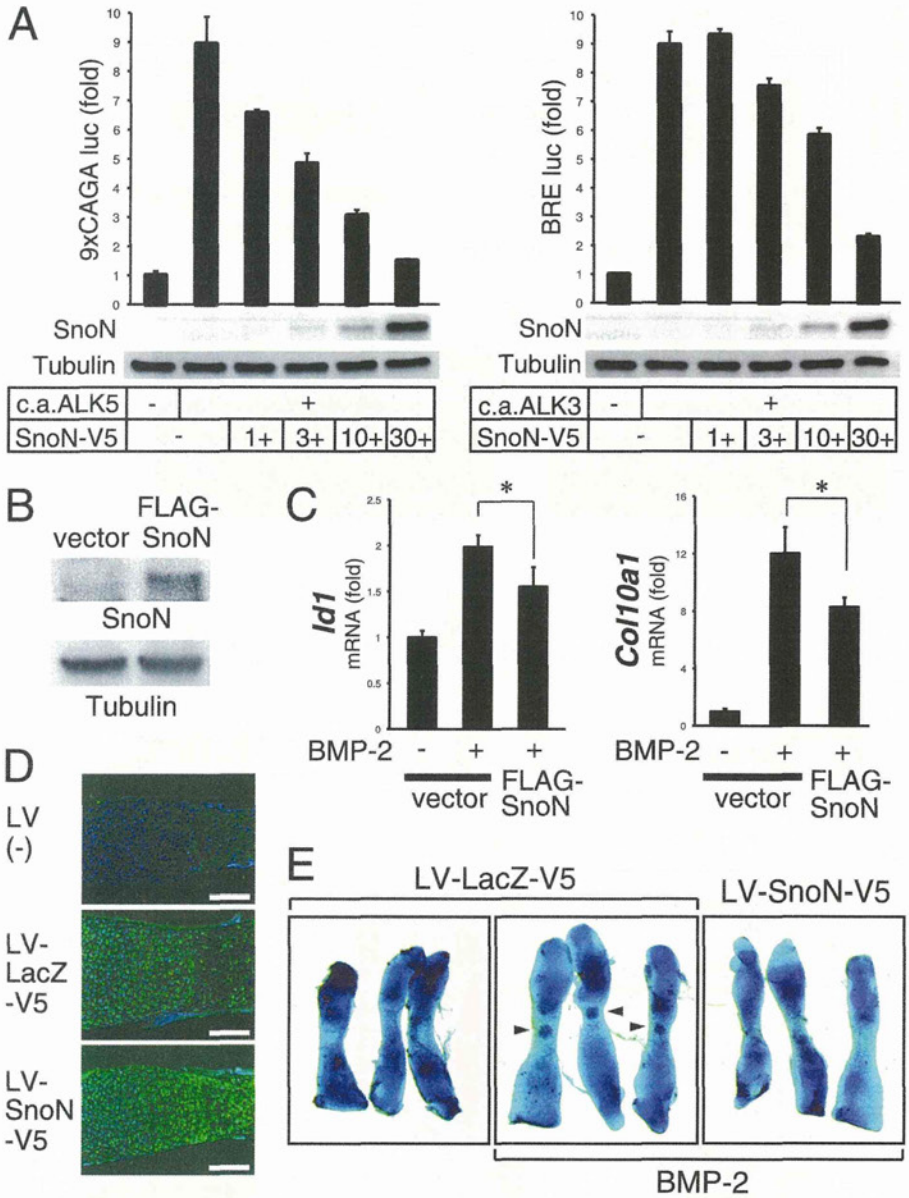

FIGURE 5. **SnoN suppresses BMP signaling and subsequent chondrocyte maturation.** *A*, SnoN expression vector was transfected with plasmids of constitutively active type I receptors and a luciferase reporter of 9xCAGA luc (for TGF-β signaling) or BRE luc (for BMP signaling) into COS-7 cells. Expression of transfected SnoN was confirmed by anti-SnoN immunoblot. Tubulin served as loading control. *B*, FLAG-tagged SnoN expression vector was stably transfected into ATDC5 chondrocytes, and its expression was confirmed by anti-SnoN immunoblotting. *C*, SnoN suppressed expression of *Id1* as well as *Col10a1* at day 7 of BMP-2 (300 ng/ml) treatment in a stable transfectant of ATDC5 chondrocytes. *D* and *E*, metatarsal bones of E17.5 mouse embryo were infected with indicated lentivirus (*LV*) for 16 h. Immunostaining using FITC-linked anti-V5 antibody on bone coronal sections was performed at day 2 of culture to evaluate the efficiency of lentiviral infection. Nuclei were stained with Hoechst dye. Merged images are presented. LV-LacZ-V5 served as a lentiviral infection control (*D*). *Scale bars*, 200 μm. Alcian blue/alizarin red staining was performed at day 2 of BMP-2 treatment (*E*). The *arrowheads* indicate the calcified cartilage matrix in bone rudiments of triplicate culture. *, $p < 0.05$. *Error bars*, S.D.

SnoN Suppresses the BMP-Smad Signaling Pathway to Inhibit Hypertrophic Maturation of Chondrocytes—SnoN interacts with Smad2, Smad3, and Smad4 in the cytoplasm to prevent their nuclear translocation (40, 41). In the nucleus, it represses their transcriptional activity by disrupting the active trimeric Smad complex and recruiting transcriptional corepressors (36), thereby negatively regulating TGF-β signaling. It is not known whether SnoN suppresses canonical BMP-Smad signaling in the same manner as the related family molecule c-Ski (42); however, SnoN may inhibit the pathway because of its ability to bind Smad4, although it cannot bind Smad1/5/8 (43). To test this hypothesis, SnoN was investigated using a BRE luciferase reporter specifically responding to the BMP-Smad pathway (33) in COS-7 cells. As a positive control for the SnoN function, SnoN was applied to the 9xCAGA TGF-β signal reporter (44), activated by constitutively active TGF-β type I receptor ALK5, to show a dose-dependent potent inhibition (Fig. 5*A*, *left*). Interestingly, SnoN did suppress the activity of

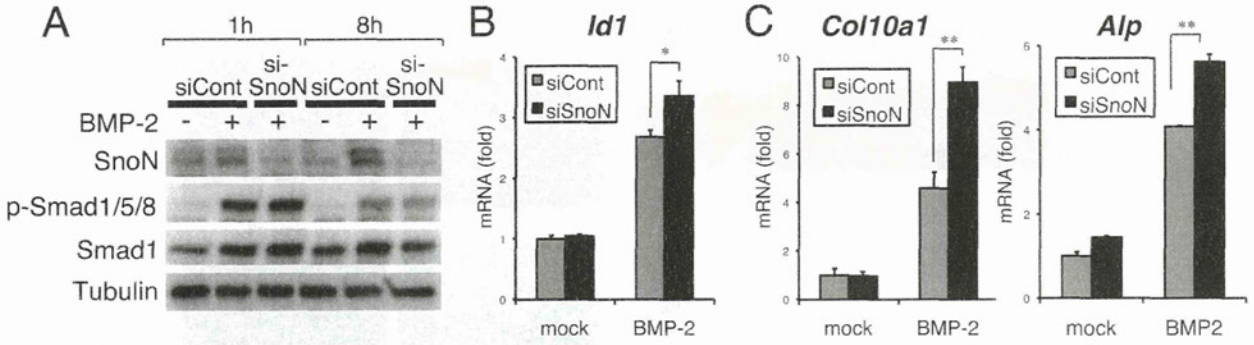

FIGURE 6. **Loss of SnoN in ATDC5 chondrocytes mimics the effect of SB431542, which accelerates the expression of *Id1* and hypertrophic marker genes.** *A*, ATDC5 cells were stimulated by BMP-2 (300 ng/ml) 16 h after transfection with siRNA. Cells harvested at the indicated time points were subjected to immunoblotting. *B* and *C*, ATDC5 chondrocytes were transfected with siRNA for 16 h, followed by induction of differentiation with BMP-2 for 3 days. Expression of *Id1*, *Col10a1*, and *Alp* was analyzed by real-time RT-PCR. *, $p < 0.05$; **, $p < 0.01$. *Error bars*, S.D.

the BRE reporter induced by the constitutively active type I BMP receptor ALK3 (encoded by *Bmpr1a*) (Fig. 5*A*, *right*) in a dose-dependent manner, although more than 3 times the amount of SnoN plasmid DNA was required for the inhibition compared with the reporter assay using 9xCAGA. Next, we stably transfected a FLAG-tagged SnoN expression vector into ATDC5 cells and confirmed the transgene expression by anti-SnoN immunoblotting (Fig. 5*B*). In ATDC5 chondrocytes, gain of SnoN suppressed the elevated expression of *Id1* at day 7 of BMP-2 induction (Fig. 5*C*, *left*). The increased expression of the hypertrophic marker *Col10a1* was also down-regulated by SnoN in BMP-treated ATDC5 cells (Fig. 5*C*, *right*). Thus, forced expression of SnoN in ATDC5 chondrocytes inhibited BMP signaling and, subsequently, chondrocyte maturation. To investigate the role of SnoN in cartilage maturation, we infected lentivirus carrying V5-tagged SnoN expression cassette into E17.5 metatarsal bone rudiments. We confirmed the infection efficiency of the lentivirus by performing immunohistochemistry on the coronal sections of the bones, using anti-V5-FITC antibody to detect the transgene product (Fig. 5*D*). In lentivirus-infected bones, we found the certain expression of V5-tagged transgenes in the cells of perichondrium and the chondrocytes in zones of reserve, proliferative, and prehypertrophic but not hypertrophic chondrocytes. Treatment of BMP-2 induced calcification of the hypertrophic zone of bone rudiments (Fig. 5*E*, *arrowheads*), whereas overexpression of SnoN by lentivirus completely prevented the cartilage mineralization (Fig. 5*E*). These data demonstrate that gain of SnoN inhibits the maturation of the hypertrophic chondrocytes.

Next, we investigated the physiological role of endogenous SnoN in ATDC5 chondrocytes by performing an siRNA-mediated knockdown assay. We confirmed that SnoN protein expression was induced upon BMP-2 induction, even at the early time points, and that the two bands (representing SnoN and SnoN2) could be efficiently eliminated by siSnoN (Fig. 6*A*). BMP-2 induced a potent phosphorylation of Smad1/5/8, whereas siSnoN showed no effect on the phosphorylation level, even after the phosphorylation declined at 8 h (Fig. 6*A*). However, knockdown of SnoN mildly, but significantly, enhanced the BMP-2-induced increase of the *Id1* gene at day 4 in ATDC5 cells (Fig. 6*B*). siSnoN further significantly enhanced the BMP-induced up-regulation of *Col10a1* as well as alkaline phosphatase (*Alp*), another marker of matured hypertrophic chondrocytes (Fig. 6*C*). These data for the SB431542-mimicking effects of siSnoN (Figs. 2 and 3) indicated that SnoN mediated a major part of the roles of endogenous TGF-β signaling in chondrocytes to physiologically suppress BMP signaling and subsequent chondrocyte hypertrophic maturation without affecting the activating step of Smad1/5/8.

TGF-β Signaling and Expression of SnoN Are Accentuated in "Prehypertrophic" Chondrocytes Adjacent to Pathologically Hypertrophic Chondrocyte in Moderately Affected OA Cartilage—Given the role of SnoN in the prevention of hypertrophic conversion of chondrocytes, SnoN protein may be present before pathologic chondrocytes gained hypertrophic phenotype in OA cartilages (8, 9). We performed immunohistochemistry assays for SnoN in human OA cartilages of various severities. In normal adult human femoral head cartilage, expression of type X collagen was entirely absent, whereas SnoN protein was weakly detected in the superficial zone (Fig. 7*A*). In moderate OA cartilage, in which the severity was graded as 6 according to the modified Mankin score (45, 46), type X collagen-positive pathologically hypertrophic chondrocytes were located in the upper layer of degenerated cartilage, which was poorly stained by Safranin O. Strikingly, we detected potent signals for SnoN protein in chondrocytes in which the cell body was mildly enlarged, resembling "prehypertrophic" chondrocytes in the developing bone. These SnoN-positive cells formed colonies located in close proximity of the colonies of hypertrophic chondrocytes (Fig. 7*A*). In severe OA cartilage of a grading score of 10, the cartilage surface of which was entirely destroyed, a few colonies of pathologically hypertrophic chondrocytes expressing type X collagen were present; however, we could no longer detect SnoN-positive cells (Fig. 7*A*). These data are consistent with our hypothesis that SnoN prevents the progression of hypertrophic conversion of articular chondrocytes. Finally, we asked if this enhanced expression of SnoN protein was associated with TGF-β signaling in human OA cartilage, similarly as observed in the growth plate of mouse embryo (Figs. 3*D* and 4*H*). In moderate OA cartilage, an immunofluorescence assay revealed the abundant accumulation of TGF-β1 protein around the "prehypertrophic" chondrocytes (Fig. 7*B*). Moreover, phosphorylated active Smad3 was detected in these pathologic chondrocytes. Again, SnoN protein was also expressed in chon-

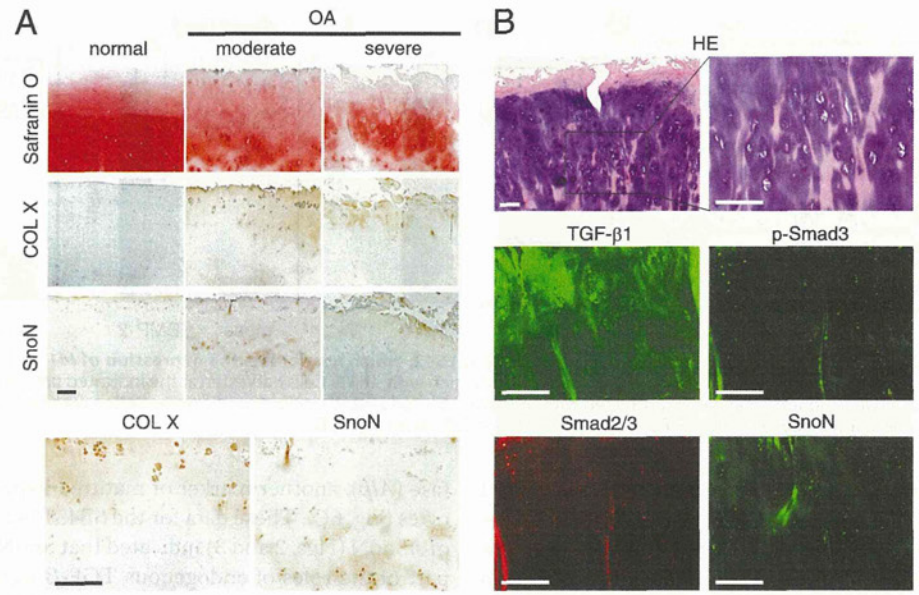

FIGURE 7. **TGF-β signaling and expression of SnoN are up-regulated in mildly hypertrophic chondrocytes located adjacent to colonies of pathologically hypertrophic chondrocytes in human OA cartilage.** *A*, human OA cartilage samples were subjected to immunohistochemistry for type X collagen (*COL X*) and SnoN. The severity of OA was graded according to the modified Mankin score on the basis of the histology of cartilage specimens stained with Safranin O. *Bottom panel*, magnified images of a moderate OA sample in the *top panel*. *B*, the human OA cartilage specimen of moderate severity was subjected to hematoxylin and eosin (*HE*) staining and immunohistochemistry for TGF-β1, phosphorylated Smad3 (*p-Smad3*), total Smad2/3, and SnoN. *Scale bars*, 200 μm.

drocytes in this region. These data demonstrated an association of TGF-β signaling and expression of SnoN in the degenerating cartilage.

DISCUSSION

Endogenous TGF-β Signaling Is Activated in Maturing Chondrocytes to Induce SnoN—Although the importance of TGF-β signaling in preventing hypertrophic conversion of chondrocytes has been demonstrated (23, 24, 47), the mode of TGF-β signaling during chondrocyte maturation and its direct target gene(s) responsible for inhibiting the differentiation remain largely unknown. While exogenously applied TGF-β has been reported to have a positive role in early chondrogenesis *in vitro*, SB431542 showed no effect on bone growth, whereas it dramatically enhanced the matrix calcification by the mature hypertrophic chondrocytes in a bone organ culture system (Fig. 1). This result suggested that endogenous TGF-β signaling was more active in the late stage of maturing chondrocytes than in the early stage of chondrocyte differentiation. Indeed, expression of *Tgfb1* was up-regulated in the late phase of differentiation of ATDC5 chondrocytes (Fig. 3*A*), coupled with an increase in phosphorylation of Smad2, which was inhibited by SB431542 (Fig. 3, *B* and *C*). This was completely linked to the expression pattern of SnoN (Fig. 4, *A–C*). SnoN expression was probably directly induced by endogenous TGF-β signaling because *SnoN* had been shown to be directly induced by TGF-β-activated Smad2 through its binding to the Smad-binding element in the promoter of the *SnoN* gene (48). Interestingly, in Smad3-deficient chondrocytes, the expression of TGF-β1, TGF-β type I receptor ALK5 (*Tgfbr1*), and SnoN was suppressed, whereas the expression of Smad1, Smad5, Smad6, BMP-2, and BMP-6 was elevated (26), suggesting SnoN to be one of the downstream targets of TGF-β signaling in chondrocytes. For the first time, we demonstrated the rapid and transient induction of *SnoN* by exogenously applied BMP ligand, whereas it was not suppressed by SB431542 (Fig. 4*F*). The *SnoN* expression pattern in the early phase, which resembled that of *Id1* (Fig. 4*F*), led us to hypothesize that the BMP-Smad pathway, in addition to TGF-β-Smad signaling, can directly induce *SnoN* in a context-dependent manner. Indeed, the sequences of GGCACC or GGCGCG, both of which contain a 1-base mismatch with the BMP-Smad-responsive motif GGCGCC (33), can be found adjacent to three TGF-β-responsive CAGA Smad-binding elements in the *SnoN* promoter (48). Further experiments are required to resolve this hypothesis and to evaluate the roles of BMP-Smad-induced SnoN.

SnoN Interferes with BMP Signaling to Suppress Hypertrophic Differentiation of Chondrocytes—The *Sno* gene (whose name derived from "*Ski*-related novel gene") was initially discovered on the basis of its close homology to v-Ski and c-Ski. Ski proteins can suppress TGF-β signaling, as well as BMP signaling, by binding to R-Smads and Smad4. Interestingly, although c-Ski can interact weakly with Smad1/5, the strong interaction with Smad4 is indispensable for suppression of BMP signaling by c-Ski (42). Although SnoN interacts with Smad4, the role of SnoN in the context of BMP signaling has not been well investigated. We showed here that SnoN suppressed BMP signaling in a comparative but slightly weaker manner compared with TGF-β signaling (Fig. 5*A*). This weaker suppression of BMP signaling is probably due to the difference in the accessibility to Smads (*i.e.* SnoN could bind to Smad2/3 and Smad4 but not to Smad1/5, unlike c-Ski) (43). Loss of SnoN mildly enhanced the expression of *Id1*, whereas it did not affect the phosphorylation level of Smad1/5/8 (Fig. 6, *A* and *B*), supporting the notion that the functional molecular target of SnoN was not the phosphor-

ylation step of Smad1/5/8 but rather Smad4. Because siSnoN and SB431542 showed an essentially similar effect with regard to phospho-Smad1/5/8 and *Id1* expression (compare Fig. 3, *E* and *F*, and Fig. 6, *A* and *B*), SnoN seems to be one of the major mediators of TGF-β signaling to inhibit BMP signaling in chondrocytes. This is interesting because we previously reported a similar negative feedback mechanism regulated by signal cross-talk between TGF-β and BMP signaling in osteoblast differentiation, in which I-Smads were induced by endogenous TGF-β signaling to inhibit BMP signaling in the maturation phase (49). However, the expression of I-Smads was not dramatically affected by SB431542 in ATDC5 chondrocytes (supplemental Fig. 1), suggesting context-dependent mechanisms in the selection of TGF-β target genes in these mesenchymal cells. The effect of forced expression, or knockdown, of SnoN showed more dramatic changes in the *Col10a1* expression than in that of *Id1* (Figs. 5*C* and 6*C*). The persistently mild suppression of BMP signaling by SnoN during the maturing phase may account for the major inhibition of hypertrophic maturation of chondrocytes.

Expression of SnoN Is Associated with the Enhanced TGF-β Signaling in Prehypertrophic Chondrocytes in Mouse Developing Bone and Human OA Cartilage—Maintenance of the articular cartilage depends on the function of articular chondrocytes, which produce cartilage matrix and are constrained from undergoing the maturation program seen in growth plate chondrocytes of developing bone. Genetic association of single nucleotide polymorphisms (SNPs) in the *SMAD3* or *ASPN* gene (encoding asporin) with human OA has been reported (50, 51). Asporin was shown to bind TGF-β ligands on the cell surface to block their signal transduction (52). In articular cartilage of old mice, decreased expression of TGF-β ligands and receptors, coupled with strongly dropped phosphorylation of Smad2, was observed (53). Moreover, as mentioned in the Introduction, mouse models of loss of TGF-β signaling showed an OA phenotype with accelerated hypertrophic conversion of chondrocytes. These lines of evidence clearly demonstrate the importance of TGF-β signaling in preventing OA change of articular chondrocytes. To date, the mechanism by which TGF-β signaling regulates this process is largely unknown. One candidate for targeting TGF-β signaling is Smurf2, a protein whose expression was up-regulated in human OA cartilage, whereas forced expression of Smurf2 in chondrocytes developed OA change in joints of the transgenic mice (25). Because Smurf2 is a TGF-β-inducible molecule to inhibit TGF-β signaling, it may mediate the effect of TGF-β signaling in chondrocyte hypertrophy. However, in *Smad3*-deficient chondrocytes, which showed enhanced BMP signaling and accelerated maturation, expression of *Smurf2* was not affected (26). Similarly, in our ATDC5 micromass culture system, *Smurf2* was not elevated in maturing ATDC5 chondrocytes stimulated by BMP-2 (supplemental Fig. 1). In contrast, we detected an increase of SnoN expression, not only in both maturing ATDC5 cells and primary chondrocytes *in vitro* but also in prehypertrophic chondrocytes in mouse developing bone and in human OA cartilage (Figs. 4 and 7). Although we demonstrated the inhibitory role of SnoN in chondrocyte hypertrophy *in vitro* (Figs. 5 and 6), hypertrophy of chondrocytes was present in both developing normal mouse cartilage and degenerating human OA cartilage, despite the accentuated expression of SnoN in contiguous prehypertrophic chondrocytes (Figs. 4*H* and 7). In mouse E17.5 bone, phosphorylation of Smad2 and expression of SnoN were diminished in hypertrophic chondrocytes despite the abundant accumulation of TGF-β1 protein in the extracellular matrix (Figs. 3*D* and 4*H*), suggesting a disorder of the signal transduction by unknown mechanisms to be resolved. Similarly, in human OA cartilage, expression of SnoN was weakened in colonies of COL X-positive hypertrophic cells (Fig. 7*A*). Taken together, it is likely that the hypertrophic conversion was induced after the decline of SnoN expression in these chondrocytes. In this regard, further investigation is required to understand why the transduction of TGF-β signaling and subsequent expression of SnoN are diminished in hypertrophic chondrocytes. Although our results do not establish an etiologic role for SnoN in the progression of OA, they at least establish a strong association that explains a possible causal relationship between SnoN regulation and hypertrophic conversion of chondrocytes in OA cartilage. Loss of SnoN in mice *in vivo* should reveal its putative roles in cartilage hypertrophy or endochondral ossification; however, SnoN knock-out mice showed embryonic lethality at E3.5 (39). Therefore, a conditional knock-out mouse line of chondrocyte-specific ablation of the *SnoN* gene would be suitable to address these questions. In conclusion, our data revealed a novel role of SnoN in regulating BMP signaling and subsequent chondrocyte maturation as a downstream mediator of TGF-β signaling. SnoN may be targeted in chondrocytes to inhibit its function in order to accelerate endochondral ossification or to enhance its activity in the case of treating OA or cartilage regeneration for repair.

Acknowledgment—We gratefully acknowledge the technical assistance of Hui Gao.

REFERENCES

1. Akiyama, H., Chaboissier, M. C., Martin, J. F., Schedl, A., and de Crombrugghe, B. (2002) The transcription factor Sox9 has essential roles in successive steps of the chondrocyte differentiation pathway and is required for expression of Sox5 and Sox6. *Genes Dev.* **16,** 2813–2828
2. Provot, S., and Schipani, E. (2005) Molecular mechanisms of endochondral bone development. *Biochem. Biophys. Res. Commun.* **328,** 658–665
3. Enomoto, H., Enomoto-Iwamoto, M., Iwamoto, M., Nomura, S., Himeno, M., Kitamura, Y., Kishimoto, T., and Komori, T. (2000) Cbfa1 is a positive regulatory factor in chondrocyte maturation. *J. Biol. Chem.* **275,** 8695–8702
4. Zheng, Q., Zhou, G., Morello, R., Chen, Y., Garcia-Rojas, X., and Lee, B. (2003) Type X collagen gene regulation by Runx2 contributes directly to its hypertrophic chondrocyte-specific expression *in vivo*. *J. Cell Biol.* **162,** 833–842
5. Ueta, C., Iwamoto, M., Kanatani, N., Yoshida, C., Liu, Y., Enomoto-Iwamoto, M., Ohmori, T., Enomoto, H., Nakata, K., Takada, K., Kurisu, K., and Komori, T. (2001) Skeletal malformations caused by overexpression of Cbfa1 or its dominant negative form in chondrocytes. *J. Cell Biol.* **153,** 87–100
6. Takeda, S., Bonnamy, J. P., Owen, M. J., Ducy, P., and Karsenty, G. (2001) Continuous expression of Cbfa1 in nonhypertrophic chondrocytes uncovers its ability to induce hypertrophic chondrocyte differentiation and partially rescues Cbfa1-deficient mice. *Genes Dev.* **15,** 467–481
7. Scotti, C., Tonnarelli, B., Papadimitropoulos, A., Scherberich, A., Schaeren, S., Schauerte, A., Lopez-Rios, J., Zeller, R., Barbero, A., and Martin, I.

(2010) Recapitulation of endochondral bone formation using human adult mesenchymal stem cells as a paradigm for developmental engineering. *Proc. Natl. Acad. Sci. U.S.A.* **107,** 7251–7256
8. Pullig, O., Weseloh, G., Ronneberger, D., Käkönen, S., and Swoboda, B. (2000) Chondrocyte differentiation in human osteoarthritis. Expression of osteocalcin in normal and osteoarthritic cartilage and bone. *Calcif. Tissue Int.* **67,** 230–240
9. Sandell, L. J., and Aigner, T. (2001) Articular cartilage and changes in arthritis. An introduction. Cell biology of osteoarthritis. *Arthritis Res.* **3,** 107–113
10. Dreier, R. (2010) Hypertrophic differentiation of chondrocytes in osteoarthritis. The developmental aspect of degenerative joint disorders. *Arthritis Res. Ther.* **12,** 216
11. Nelea, V., Luo, L., Demers, C. N., Antoniou, J., Petit, A., Lerouge, S., R Wertheimer, M., and Mwale, F. (2005) Selective inhibition of type X collagen expression in human mesenchymal stem cell differentiation on polymer substrates surface-modified by glow discharge plasma. *J. Biomed. Mater. Res. A* **75,** 216–223
12. Sekiya, I., Vuoristo, J. T., Larson, B. L., and Prockop, D. J. (2002) *In vitro* cartilage formation by human adult stem cells from bone marrow stroma defines the sequence of cellular and molecular events during chondrogenesis. *Proc. Natl. Acad. Sci. U.S.A.* **99,** 4397–4402
13. Miyazono, K., Kamiya, Y., and Morikawa, M. (2010) Bone morphogenetic protein receptors and signal transduction. *J. Biochem.* **147,** 35–51
14. Tsumaki, N., Nakase, T., Miyaji, T., Kakiuchi, M., Kimura, T., Ochi, T., and Yoshikawa, H. (2002) Bone morphogenetic protein signals are required for cartilage formation and differently regulate joint development during skeletogenesis. *J. Bone Miner. Res.* **17,** 898–906
15. Yoon, B. S., Ovchinnikov, D. A., Yoshii, I., Mishina, Y., Behringer, R. R., and Lyons, K. M. (2005) Bmpr1a and Bmpr1b have overlapping functions and are essential for chondrogenesis *in vivo*. *Proc. Natl. Acad. Sci. U.S.A.* **102,** 5062–5067
16. Retting, K. N., Song, B., Yoon, B. S., and Lyons, K. M. (2009) BMP canonical Smad signaling through Smad1 and Smad5 is required for endochondral bone formation. *Development* **136,** 1093–1104
17. Furumatsu, T., Tsuda, M., Taniguchi, N., Tajima, Y., and Asahara, H. (2005) Smad3 induces chondrogenesis through the activation of SOX9 via CREB-binding protein/p300 recruitment. *J. Biol. Chem.* **280,** 8343–8350
18. Volk, S. W., Luvalle, P., Leask, T., and Leboy, P. S. (1998) A BMP-responsive transcriptional region in the chicken type X collagen gene. *J. Bone Miner. Res.* **13,** 1521–1529
19. Leboy, P., Grasso-Knight, G., D'Angelo, M., Volk, S. W., Lian, J. V., Drissi, H., Stein, G. S., and Adams, S. L. (2001) Smad-Runx interactions during chondrocyte maturation. *J. Bone Joint Surg. Am.* **83-A,** Suppl. 1, S15–S22
20. Kempf, H., Ionescu, A., Udager, A. M., and Lassar, A. B. (2007) Prochondrogenic signals induce a competence for Runx2 to activate hypertrophic chondrocyte gene expression. *Dev. Dyn.* **236,** 1954–1962
21. Kobayashi, T., Lyons, K. M., McMahon, A. P., and Kronenberg, H. M. (2005) BMP signaling stimulates cellular differentiation at multiple steps during cartilage development. *Proc. Natl. Acad. Sci. U.S.A.* **102,** 18023–18027
22. van Beuningen, H. M., Glansbeek, H. L., van der Kraan, P. M., and van den Berg, W. B. (1998) Differential effects of local application of BMP-2 or TGF-β1 on both articular cartilage composition and osteophyte formation. *Osteoarthr. Cartil.* **6,** 306–317
23. Yang, X., Chen, L., Xu, X., Li, C., Huang, C., and Deng, C. X. (2001) TGF-β/Smad3 signals repress chondrocyte hypertrophic differentiation and are required for maintaining articular cartilage. *J. Cell Biol.* **153,** 35–46
24. Serra, R., Johnson, M., Filvaroff, E. H., LaBorde, J., Sheehan, D. M., Derynck, R., and Moses, H. L. (1997) Expression of a truncated, kinase-defective TGF-β type II receptor in mouse skeletal tissue promotes terminal chondrocyte differentiation and osteoarthritis. *J. Cell Biol.* **139,** 541–552
25. Wu, Q., Kim, K. O., Sampson, E. R., Chen, D., Awad, H., O'Brien, T., Puzas, J. E., Drissi, H., Schwarz, E. M., O'Keefe, R. J., Zuscik, M. J., and Rosier, R. N. (2008) Induction of an osteoarthritis-like phenotype and degradation of phosphorylated Smad3 by Smurf2 in transgenic mice. *Arthritis Rheum.* **58,** 3132–3144
26. Li, T. F., Darowish, M., Zuscik, M. J., Chen, D., Schwarz, E. M., Rosier, R. N., Drissi, H., and O'Keefe, R. J. (2006) Smad3-deficient chondrocytes have enhanced BMP signaling and accelerated differentiation. *J. Bone Miner. Res.* **21,** 4–16
27. Bobick, B. E., and Kulyk, W. M. (2004) The MEK-ERK signaling pathway is a negative regulator of cartilage-specific gene expression in embryonic limb mesenchyme. *J. Biol. Chem.* **279,** 4588–4595
28. Gosset, M., Berenbaum, F., Thirion, S., and Jacques, C. (2008) Primary culture and phenotyping of murine chondrocytes. *Nat. Protoc.* **3,** 1253–1260
29. Alvarez, J., Sohn, P., Zeng, X., Doetschman, T., Robbins, D. J., and Serra, R. (2002) TGFβ2 mediates the effects of hedgehog on hypertrophic differentiation and PTHrP expression. *Development* **129,** 1913–1924
30. Tominaga, H., Maeda, S., Hayashi, M., Takeda, S., Akira, S., Komiya, S., Nakamura, T., Akiyama, H., and Imamura, T. (2008) CCAAT/enhancer-binding protein β promotes osteoblast differentiation by enhancing Runx2 activity with ATF4. *Mol. Biol. Cell* **19,** 5373–5386
31. Ahrens, P. B., Solursh, M., and Reiter, R. S. (1977) Stage-related capacity for limb chondrogenesis in cell culture. *Dev. Biol.* **60,** 69–82
32. Shukunami, C., Ohta, Y., Sakuda, M., and Hiraki, Y. (1998) Sequential progression of the differentiation program by bone morphogenetic protein-2 in chondrogenic cell line ATDC5. *Exp. Cell Res.* **241,** 1–11
33. Korchynskyi, O., and ten Dijke, P. (2002) Identification and functional characterization of distinct critically important bone morphogenetic protein-specific response elements in the Id1 promoter. *J. Biol. Chem.* **277,** 4883–4891
34. Canalis, E., Economides, A. N., and Gazzerro, E. (2003) Bone morphogenetic proteins, their antagonists, and the skeleton. *Endocr. Rev.* **24,** 218–235
35. Miyazono, K., Maeda, S., and Imamura, T. (2005) BMP receptor signaling. Transcriptional targets, regulation of signals, and signaling cross-talk. *Cytokine Growth Factor Rev.* **16,** 251–263
36. Stroschein, S. L., Wang, W., Zhou, S., Zhou, Q., and Luo, K. (1999) Negative feedback regulation of TGF-β signaling by the SnoN oncoprotein. *Science* **286,** 771–774
37. Sun, Y., Liu, X., Ng-Eaton, E., Lodish, H. F., and Weinberg, R. A. (1999) SnoN and Ski protooncoproteins are rapidly degraded in response to transforming growth factor β signaling. *Proc. Natl. Acad. Sci. U.S.A.* **96,** 12442–12447
38. Pearson-White, S., and Crittenden, R. (1997) Proto-oncogene Sno expression, alternative isoforms and immediate early serum response. *Nucleic Acids Res.* **25,** 2930–2937
39. Shinagawa, T., Dong, H. D., Xu, M., Maekawa, T., and Ishii, S. (2000) The *sno* gene, which encodes a component of the histone deacetylase complex, acts as a tumor suppressor in mice. *EMBO J.* **19,** 2280–2291
40. Jahchan, N. S., You, Y. H., Muller, W. J., and Luo, K. (2010) Transforming growth factor-β regulator SnoN modulates mammary gland branching morphogenesis, postlactational involution, and mammary tumorigenesis. *Cancer Res.* **70,** 4204–4213
41. Krakowski, A. R., Laboureau, J., Mauviel, A., Bissell, M. J., and Luo, K. (2005) Cytoplasmic SnoN in normal tissues and nonmalignant cells antagonizes TGF-β signaling by sequestration of the Smad proteins. *Proc. Natl. Acad. Sci. U.S.A.* **102,** 12437–12442
42. Takeda, M., Mizuide, M., Oka, M., Watabe, T., Inoue, H., Suzuki, H., Fujita, T., Imamura, T., Miyazono, K., and Miyazawa, K. (2004) Interaction with Smad4 is indispensable for suppression of BMP signaling by c-Ski. *Mol. Biol. Cell* **15,** 963–972
43. Wang, W., Mariani, F. V., Harland, R. M., and Luo, K. (2000) Ski represses bone morphogenic protein signaling in *Xenopus* and mammalian cells. *Proc. Natl. Acad. Sci. U.S.A.* **97,** 14394–14399
44. Dennler, S., Itoh, S., Vivien, D., ten Dijke, P., Huet, S., and Gauthier, J. M. (1998) Direct binding of Smad3 and Smad4 to critical TGF β-inducible elements in the promoter of human plasminogen activator inhibitor-type 1 gene. *EMBO J.* **17,** 3091–3100
45. Mankin, H. J., Dorfman, H., Lippiello, L., and Zarins, A. (1971) Biochemical and metabolic abnormalities in articular cartilage from osteo-arthritic

human hips. II. Correlation of morphology with biochemical and metabolic data. *J. Bone Joint Surg. Am.* **53,** 523–537
46. Kuroki, H., Nakagawa, Y., Mori, K., Ohba, M., Suzuki, T., Mizuno, Y., Ando, K., Takenaka, M., Ikeuchi, K., and Nakamura, T. (2004) Acoustic stiffness and change in plug cartilage over time after autologous osteochondral grafting. Correlation between ultrasound signal intensity and histological score in a rabbit model. *Arthritis Res. Ther.* **6,** R492–R504
47. Li, T. F., Gao, L., Sheu, T. J., Sampson, E. R., Flick, L. M., Konttinen, Y. T., Chen, D., Schwarz, E. M., Zuscik, M. J., Jonason, J. H., and O'Keefe, R. J. (2010) Aberrant hypertrophy in Smad3-deficient murine chondrocytes is rescued by restoring transforming growth factor β-activated kinase 1/activating transcription factor 2 signaling. A potential clinical implication for osteoarthritis. *Arthritis Rheum.* **62,** 2359–2369
48. Zhu, Q., Pearson-White, S., and Luo, K. (2005) Requirement for the SnoN oncoprotein in transforming growth factor β-induced oncogenic transformation of fibroblast cells. *Mol. Cell Biol.* **25,** 10731–10744
49. Maeda, S., Hayashi, M., Komiya, S., Imamura, T., and Miyazono, K. (2004) Endogenous TGF-β signaling suppresses maturation of osteoblastic mesenchymal cells. *EMBO J.* **23,** 552–563
50. Valdes, A. M., Spector, T. D., Tamm, A., Kisand, K., Doherty, S. A., Dennison, E. M., Mangino, M., Tamm, A., Kerna, I., Hart, D. J., Wheeler, M., Cooper, C., Lories, R. J., Arden, N. K., and Doherty, M. (2010) Genetic variation in the SMAD3 gene is associated with hip and knee osteoarthritis. *Arthritis Rheum.* **62,** 2347–2352
51. Kizawa, H., Kou, I., Iida, A., Sudo, A., Miyamoto, Y., Fukuda, A., Mabuchi, A., Kotani, A., Kawakami, A., Yamamoto, S., Uchida, A., Nakamura, K., Notoya, K., Nakamura, Y., and Ikegawa, S. (2005) An aspartic acid repeat polymorphism in asporin inhibits chondrogenesis and increases susceptibility to osteoarthritis. *Nat. Genet.* **37,** 138–144
52. Nakajima, M., Kizawa, H., Saitoh, M., Kou, I., Miyazono, K., and Ikegawa, S. (2007) Mechanisms for asporin function and regulation in articular cartilage. *J. Biol. Chem.* **282,** 32185–32192
53. Blaney Davidson, E. N., Scharstuhl, A., Vitters, E. L., van der Kraan, P. M., and van den Berg, W. B. (2005) Reduced transforming growth factor-β signaling in cartilage of old mice. Role in impaired repair capacity. *Arthritis Res. Ther.* **7,** R1338–R1347

OPEN ACCESS Freely available online

PLoS one

RBPJ Is a Novel Target for Rhabdomyosarcoma Therapy

Hiroko Nagao[1,2], Takao Setoguchi[2]*, Sho Kitamoto[3], Yasuhiro Ishidou[4], Satoshi Nagano[1], Masahiro Yokouchi[1], Masahiko Abematsu[1,2], Naoya Kawabata[1], Shingo Maeda[4], Suguru Yonezawa[3], Setsuro Komiya[1]

1 Department of Orthopaedic Surgery, Graduate School of Medical and Dental Sciences, Kagoshima University, Kagoshima, Japan, **2** The Near-Future Locomotor Organ Medicine Creation Course (Kusunoki Kai), Graduate School of Medical and Dental Sciences, Kagoshima University, Kagoshima, Japan, **3** Department of Human Pathology, Field of Oncology, Graduate School of Medical and Dental Sciences, Kagoshima University, Kagoshima, Japan, **4** Department of Medical Joint Materials, Graduate School of Medical and Dental Sciences, Kagoshima University, Kagoshima, Japan

Abstract

The Notch pathway regulates a broad spectrum of cell fate decisions and differentiation processes during fetal and postnatal development. In addition, the Notch pathway plays an important role in controlling tumorigenesis. However, the role of *RBPJ*, a transcription factor in the Notch pathway, in the development of tumors is largely unknown. In this study, we focused on the role of *RBPJ* in the pathogenesis of rhabdomyosarcoma (RMS). Our data showed that Notch pathway genes were upregulated and activated in human RMS cell lines and patient samples. Inhibition of the Notch pathway by a γ-secretase inhibitor (GSI) decreased the *in vitro* proliferation of RMS cells. Knockdown of *RBPJ* expression by RNAi inhibited the anchorage-independent growth of RMS cells and the growth of xenografts *in vivo*. Additionally, overexpression of *RBPJ* promoted the anchorage-independent growth of RMS cells. Further, we revealed that *RBPJ* regulated the cell cycle in RMS xenograft tumors and decreased proliferation. Our findings suggest that *RBPJ* regulates the RMS growth, and that the inhibition of *RBPJ* may be an effective therapeutic approach for patients with RMS.

Citation: Nagao H, Setoguchi T, Kitamoto S, Ishidou Y, Nagano S, et al. (2012) RBPJ Is a Novel Target for Rhabdomyosarcoma Therapy. PLoS ONE 7(7): e39268. doi:10.1371/journal.pone.0039268

Editor: Qiang Wang, Cedars-Sinai Medical Center, United States of America

Received March 1, 2012; **Accepted** May 22, 2012; **Published** July 9, 2012

Funding: This work was supported by Grants-in-Aid for Scientific Research (KAKENHI) (C) 19591725, (C) 20591786, (C) 21591919, (C) 21591920, (C) 22591663, (C) 24592238 and (C)23592195 and a Grant-in-Aid from the Ministry of Health, Labour, and Welfare of Japan for the Third Term Comprehensive Control Research for Cancer, and Scientific Research on Priority Areas 201201976 to HN from the Grant-in-Aid for JSPS Fellow. The funders had no role in study design, data collection and analysis, decision to publish, or preparation of the manuscript.

Competing Interests: The authors have declared that no competing interests exist.

* E-mail: setoro@m2.kufm.kagoshima-u.ac.jp

Introduction

Rhabdomyosarcoma (RMS) is the most common soft tissue sarcoma in children and adolescents [1,2,3]. Pediatric RMS can be divided into 2 major subtypes, embryonal RMS (eRMS) and alveolar RMA (aRMS). The cure rates for patients with nonmetastatic RMS have improved significantly from an estimated 25% in 1970 to 75% at present. Prognosis for RMS is dependent on the anatomic site of the primary tumor, age, completeness of resection, presence and the number of metastatic sites, and histological and biological characteristics of the tumor cells [4,5]. The advances in the understanding of tumor biology may lead to the development of novel clinically relevant therapeutic targets in the near future.

The Notch signaling cascade is highly conserved and plays a crucial role in the self-renewal of stem cells, cell fate determination, epithelial cell polarity, adhesion, cell division, and apoptosis [6,7,8]. The mammalian family of Notch receptors consists of 4 members (*NOTCH1-4*) and the ligand family consists of 5 members (*JAGGED 1/2* and *DELTA 1/3/4*). In the absence of ligand binding, the Notch receptors are inactive. Upon ligand binding, the Notch receptor is cleaved in 2 sequential steps. The cleavage events release the intracellular domain of the Notch receptor (NICD), and the NICD regulates the downstream target genes via the DNA-binding factor, *RBPJ/CBF1* [9,10]. The transcriptional regulator *RBPJ* is a highly conserved DNA-binding protein that plays a central role in canonical Notch signaling [11].

Recently, alterations in the Notch pathway have been observed in different solid tumors, including breast cancer, ovarian cancer, melanoma, glioblastoma, and lung and pancreatic cancer [12,13,14]. In addition, aberrant activation of the Notch-RBPJ pathway is involved in Epstein–Barr virus (EBV) infection [15,16], T-lymphoblastic leukemia (T-LL), and gliomas [17,18].

We previously reported that inhibition of the Notch pathway suppressed the growth of osteosarcoma by regulation of cell cycle [19]. In this study, we found that the Notch pathway was also functionally activated in human RMS, and a γ-secretase inhibitor (GSI) X reduced the *in vitro* proliferation of RMS cells. Moreover, we show that inhibition of *RBPJ* expression prevents the growth of RMS *in vitro* and *in vivo*.

Materials and Methods

Cell Lines

RD and KYM-1 cell lines were obtained from the Health Science Research Resources Bank (HSRRB, Osaka, Japan). RMS-YM cell line was obtained from Riken Bioresource Center (Tsukuba, Japan). HSKMc cell line was purchased from TOYOBO (Osaka, Japan). RD and KYM-1 cell lines were cultured in Dulbecco's modified Eagle's medium (DMEM)

supplemented with 10% fetal bovine serum (FBS), 100 U/mL penicillin, and 100 μg/mL streptomycin. RMS-YM cell line was cultured in RPMI 1640 medium supplemented with 10% FBS, 100 μM nonessential amino acids (NEAA), 20 mM HEPES, 100 U/mL penicillin, and 100 μg/mL streptomycin. HSKMc cell line was cultured in skeletal muscle cell growth medium (TOYOBO, Osaka, Japan). All cells were maintained at 37°C in 5% CO_2.

Patient Specimens

Human eRMS biopsy specimens were collected from primary lesions before any diagnostic or therapeutic treatment. Human skeletal muscle tissues were collected from patients undergoing operation for scoliosis. The study protocol was approved by the institutional Review Board of Kagoshima University. Informed consent was obtained from all patients.

Real-time PCR Analysis

Real-time PCR analysis was performed as previously described [20]. Total RNA was extracted from cell lines and tissue specimens using miR-Vana RNA isolation kit or TRIzol (Invitrogen, CA, USA) and was reverse transcribed using ReverTra Ace -α- (TOYOBO, Osaka, Japan). cDNA was amplified by real-time PCR using SYBR Green (Life Technologies, NY, USA). Real-time PCR was performed on MiniOpticon^{TM} (Bio-Rad, Tokyo, Japan). The comparative Ct (ΔΔCt) analysis was performed to evaluate the fold change of mRNA expression, using the expression of *ACTB* as a reference. All PCR reactions were performed in triplicate. All primers were designed. using Primer 3 software. The following primers were used: *ACTB*, 5′-AGAAAATCTGGCACCACACC-3′ and 5-AGAGGCGTACAGGGATAGCA-3′; *NOTCH1*, 5′-GTGACTGCTCCCTCAACTTCAAT-3′ and 5′-CTGTCACAGTGGCCGTCACT-3′; *NOTCH2*, 5′-GTGTCAGAATGGAGGGGTTTG-3′ and 5′-ATTGCGGTTGGCACAGG-3′; *NOTCH3*, 5′-CAACCCGGTGTACGAGAAGT-3′ and 5′-GAACGCAGTAGCTCCTCTGG-3′; *NOTCH4*, 5′-CCATTGACACCCAGCTTCTT-3′ and 5-GCTGAACAGAAGTCCCGAAG-3′; *JAG1*, 5′-CAGATTTCCTTGTTCCCTTGCT-3′ and 5′-CGTTGTTGGTGGTGTTGTCC-3′; *DLL1*, 5′-CCTACTGCACAGAGCCGATCT-3′ and 5′-GCAGGTGGCTCCATTCTTGC-3′; *HES1*, 5′-AGGCGGACATTCTGGAAATG-3′ and 5′-CGGTACTTCCCCAGCACACTT-3′; *HEY1*, 5′-CGAGGTGGAGAAGGAGAGTG-3′ and 5′-CTGGGTACCAGCCTTCTCAG-3′; *RBPJ*, 5′-CGCATTATTGGATGCAGATG-3′ and 5′-CAGGAAGCGCCATCATTTAT-3′; *Cyclin D*, 5′-CAGAAGTGCGAGGAGGAGGT-3′, and 5′-CGGATGGAGTTGTCGGTGT-3′; *Cyclin E*, 5′-CCACACCTGACAAAGAAGATGATGAC-3′ and 5′-GAGCCTCTGGATGGTGCAATAAT-3′; *E2F1*, 5′-ATGTTTTCCTGTGCCCTGAG-3′ and 5′-ATCTGTGGTGAGGGATGAGG-3′; *SKP2*, 5′-TGGGAATCTTTTCCTGTCTG-3′ and 5′-GAACACTGAGACAGTATGCC-3′; *p21*, 5′-GACACCACTGGAGGGTGACT-3′ and 5′-ACAGGTCCACATGGTCTTCC-3′.

Cell Proliferation Assay

Cell proliferation assay was performed as previously described [21]. We seeded 1×10^3 cells (RD) or 3×10^3 cells (KYM-1)/100 μL in a 96 -well plate. Next day, the cells were placed in fresh medium containing the indicated concentration of the GSI X (CALBIOCHEM, Basel, Switzerland), GSI XX (CALBIOCHEM, Basel, Switzerland) or DMSO and were cultured for 3–4 days. Cell growth were measured daily by performing WST-1 assay (Roche, Basel, Switzerland).

Plasmid Constructs and Gene Transfer

Control siRNA (S20C-0600) was purchased from B-Bridge International (Cupertino, USA) and RBPJ siRNA (sc-38214) was purchased from Santa Cruz Biotechnology (CA, USA). All siRNA transfection experiments were performed using Lipofectamine RNAiMAX (Invitrogen, CA, USA) transfection reagent according to the manufacturer's protocol. Control or RBPJ shRNA (KH06319P) were purchased from SuperArray Biosciences (MD, USA). pCMV6-Entry Vector (PS100001) and RBPJ expression vector (RC204791) were purchased from Origene (Maryland, USA). All plasmid transfection experiments were performed using FuGENE6 (Roche, Basal, Switzerland) transfection reagent according to the manufacturer's protocol. Tranfected cells were selected in 700 μg/mL neomycin or 0.4 ng/μL puromycin. Stable cell lines were then used for colony formation assay and in vivo experiments.

Colony Formation Assay

Colony formation assay was performed as previously described [22]. Cells were suspended in DMEM containing 0.33% soft agar and 5% FBS and then were plated on a 0.5% soft agar layer. Cells were cultured at a density of 2×10^4 cells per well in 6-well plates. After 2–3 weeks (RBPJ siRNA/RD: 2 weeks, RBPJ/RD: 3 weeks), the number of colonies was counted. Every experiment was performed in triplicate, and all experiments were performed 3 times.

Western Blotting Analysis

Western blotting analysis was performed as previously described [23].

Cells were lysed using NP40 buffer, including 0.5% NP40, 10 mM Tris-HCl (pH 7.4), 150 mM NaCl, 3 mM pAPMSF (Wako Chemicals, Kanagawa, Japan), 5 mg/mL aprotinin (Sigma, StLouis, USA), 2 mM sodium orthovanadate (Wako Chemicals, Kanagawa, Japan), and 5 mM EDTA. Lysates were boiled with sodium dodecyl sulfate (SDS) sample buffer, separated by SDS-polyacrylamide gel electrophoresis (PAGE) (Bio-Rad, Tokyo, Japan), and transferred to a polyvinylidene fluoride (PVDF) membrane (Caliper LifeSciences, CA, USA). The membranes were blocked in 5% nonfat dry milk TBST buffer and incubated in primary antibodies diluted in TBST for 1 h at room temperature or overnight at 4°C. Blots were washed using TBST buffer and incubated with horseradish peroxidase-conjugated secondary antibodies (Cell Signaling Technology) in TBST buffer for 45 min at room temperature. Immunocomplexes were visualized using an enhanced chemiluminescence kit (GE Healthcare, Tokyo, Japan). Primary antibodies were RBPJ (1:300, ab33065, abcam), PARP (1:1000, #9542, Cell Signaling) and α-tubulin (1:1000, DM1A, Sigma-Aldrich).

Animal Studies

Xenograft experiments were performed as previously described [24]. Briefly, control or RBPJ shRNA-transfected RD cells (1×10^6) were suspended in 100 μL Matrigel (BD, NJ, USA). Cell suspensions were subcutaneously inoculated in 5-week-old nude mice (Japan SLC, Inc). Tumor size was calculated weekly using the formula $LW^2/2$ (with L and W representing the length and width of tumors). Kaplan–Meier analysis was performed using Kaplan 97 software. All animal experiments were performed in compliance with the guidelines and approved by the Animal

Science Laboratory, Frontier Science Research Center,Kagoshima University.

Immunohistochemistry

For Ki-67 staining, antigen retrieval was performed using CC1 antigen retrieval buffer (Ventana Medical Systems, Tucson, AZ, U.S.A.) for all sections. Following incubation with the primary antibody against Ki-67 (MIB-1, DAKO, dilution rate at 1:50), sections were stained on the Ventana automated slide stainer (Benchmark XT) using the Ventana diaminobenzidine detection kit (Ventana Medical Systems). Ki67 immunostainings were scored by counting at least 1000 cells in 5 randomized fields. Every stained nucleus was considered positive, irrespective of intensity.

For detection of apoptotic small bodies, cells were fixed by 4% paraformaldehyde for 20 min, washed in PBST (PBS containing 0.05% Tween20), and then permeabilized in PBS containing 0.2% Triton X-100 for 10 min. After the wash, the cells were treated with PBS containing 10 μg/mL Hoechst 33342 dye (Molecular Probes, Oregon, U.S.A) for 30 min, and then were washed. The apoptotic cells were visualized by fluorescence microscopy (Leica Microsystems, Wild Heerbrugg, Switzerland).

Statistical Analysis

All the data are expressed as mean ± SD. Statistical analysis was performed using the Student's *t* test using Microsoft Office Excel or Kaplan 97. $P<0.05$ was considered significant.

Results

Notch Pathway Genes are Upregulated in Tissue Specimens of Patients with Rhabdomyosarcoma

We assessed the status of the Notch pathway in RMS by determining the expression of genes in the Notch pathway; we performed real-time PCR to determine the expression of these genes in normal human skeletal muscle specimen and 2 human eRMS specimens. RMS1 and RMS2 showed strong expression of Notch receptors *NOTCH1*, *NOTCH3*, and *NOTCH4* in RMS specimens. Additionally, Notch ligands *JAG1* and *DLL1*, target genes *HEY1* and *HES1*, and transcription factor *RBPJ* were significantly upregulated in RMS (Fig. 1). Further, we showed that Notch pathway molecules are upregulated in RMS cell lines (Fig. S1). These findings suggest that the Notch pathway is activated in human RMS.

Downregulation of the Notch Pathway by GSI X Suppresses Rhabdomyosarcoma Cell Proliferation

To examine whether the Notch pathway contributes to RMS pathogenesis, we used GSI X and GSI XX which are potent inhibitor of Notch pathway. WST-1 assay revealed that the proliferation of RD and KYM-1 cells was inhibited by 10 μM GSI X (Fig. 2A). In addition, GSI XX prevented RD and KYM-1 proliferation (Fig. S2). We evaluated cell death by GSI X treatment. GSI X treatment did not promote the expression of cleaved PARP and formation of the apoptotic small bodies (Fig. S3). Furthermore, the Notch target gene *HES1* mRNA was downregulated by 10 μM GSI X, in RD and KYM-1 cell lines (Fig. 2B). These findings suggest that Notch pathway inhibition by GSI X treatment prevents the proliferation of RMS cells *in vitro*.

RBPJ is Essential for the Growth of Rhabdomyosarcoma

GSIs inhibit not only the Notch pathway but also other pathways [26,27,28]. We examined the function of the Notch pathway in RMS cell proliferation by analyzing the function of *RBPJ*. Real-time PCR revealed that *RBPJ* was upregulated 2.1 to 4.8-fold in RMS cell lines (Fig. 3A). To evaluate the function of *RBPJ* in RMS, we knocked down *RBPJ* expression by using siRNA. Efficacy of RNAi was confirmed by real-time PCR and western blotting assay, which showed that *RBPJ* RNAi decreased the expression of *RBPJ* mRNA and protein levels (Fig. 3B). Furthermore, knockdown of *RBPJ* decreased the expression of Notch target gene *HES1* mRNA in RD cells (Fig. 3B). RD cells transfected with *RBPJ* siRNA showed a significantly lower number of colonies in soft agar than those with control siRNA (Fig. 3C). In addition to loss-of-function of *RBPJ*, we examined the effects of forced expression of *RBPJ* in RMS cells. Forced expression of RBPJ increased the expression of downstream target gene *HES1* (Fig. 4A). The colony formation assay showed that forced expression of *RBPJ* led to formation of a greater number of colonies in soft agar than those with control vector (Fig. 4B). These findings show that *RBPJ* promotes the growth of human RMS cells *in vitro*.

Knockdown of *RBPJ* Prevents the Growth of Rhabdomyosarcoma *in vivo*

We next investigated whether knockdown of *RBPJ* affects the growth of RMS cells *in vivo*. Knockdown of *RBPJ* by transfection of *RBPJ* shRNA significantly inhibited the growth of RD xenograft in nude mice as compared to that of control shRNA-transfected xenograft (Fig. 5A). Kaplan–Meier analysis revealed that knockdown of *RBPJ* showed a statistically significant improvement in the survival of mice (Fig. 5B). To examine whether *RBPJ* knockdown reduced cell proliferation *in vivo*, we examined the expression of Ki67 and cell cycle-related genes. The number of Ki67-positive cells in *RBPJ* shRNA-transfected xenograft was significantly lower than in control shRNA-transfected xenograft (Fig. 5C). Additionally, real-time PCR showed that the expression of the cell cycle accelerators, such as *Cyclin D*, *Cyclin E*, *E2F1*, and *SKP2* was decreased in *RBPJ* shRNA-transfected xenograft. In contrast, the expression of *p21*, a negative regulator of cell cycle, was increased in *RBPJ* shRNA-transfected xenograft (Fig. 5C). These findings suggest that *RBPJ* plays a critical role in the growth of RMS by regulation of the cell cycle *in vivo*.

Discussion

The Notch pathway is involved in several cellular processes such as proliferation, differentiation, apoptosis, cell fate decision, and maintenance of stem cells [8,12,29]. The Notch pathway plays a role in many cancers [19,30,31,32].

Our findings revealed that Notch pathway molecules were upregulated in clinical samples of eRMS were consistent with those reported in previous studies. Kuroda, K. *et al.* showed that activation of the *NOTCH1-RBPJ* pathway via the *DLL1* ligand was important for myogenic differentiation [33,34]. We also found that the mRNA expression of *NOTCH1*, *DLL1*, and *RBPJ* is higher in eRMS specimens than in normal skeletal muscle specimens. Thus, the pathogenesis of RMS might be associated with the dysregulated activation of myogenic differentiation.

Recently, the Notch pathway has been reported to be highly active in human RMS [35,36]. Roma J *et al.* reported that inhibition of the Notch pathway by GSIs reduced the invasiveness and metastasis of RMS *in vitro* [35]. In addition, Belyea *et al.* reported that Notch pathway inhibition by GSI and RNAi of *NOTCH1* or *HEY1* blocked RMS tumorigenesis [36]. GSIs, which were originally used in Alzheimer's disease [37], are currently undergoing clinical trials for the treatment of several tumors

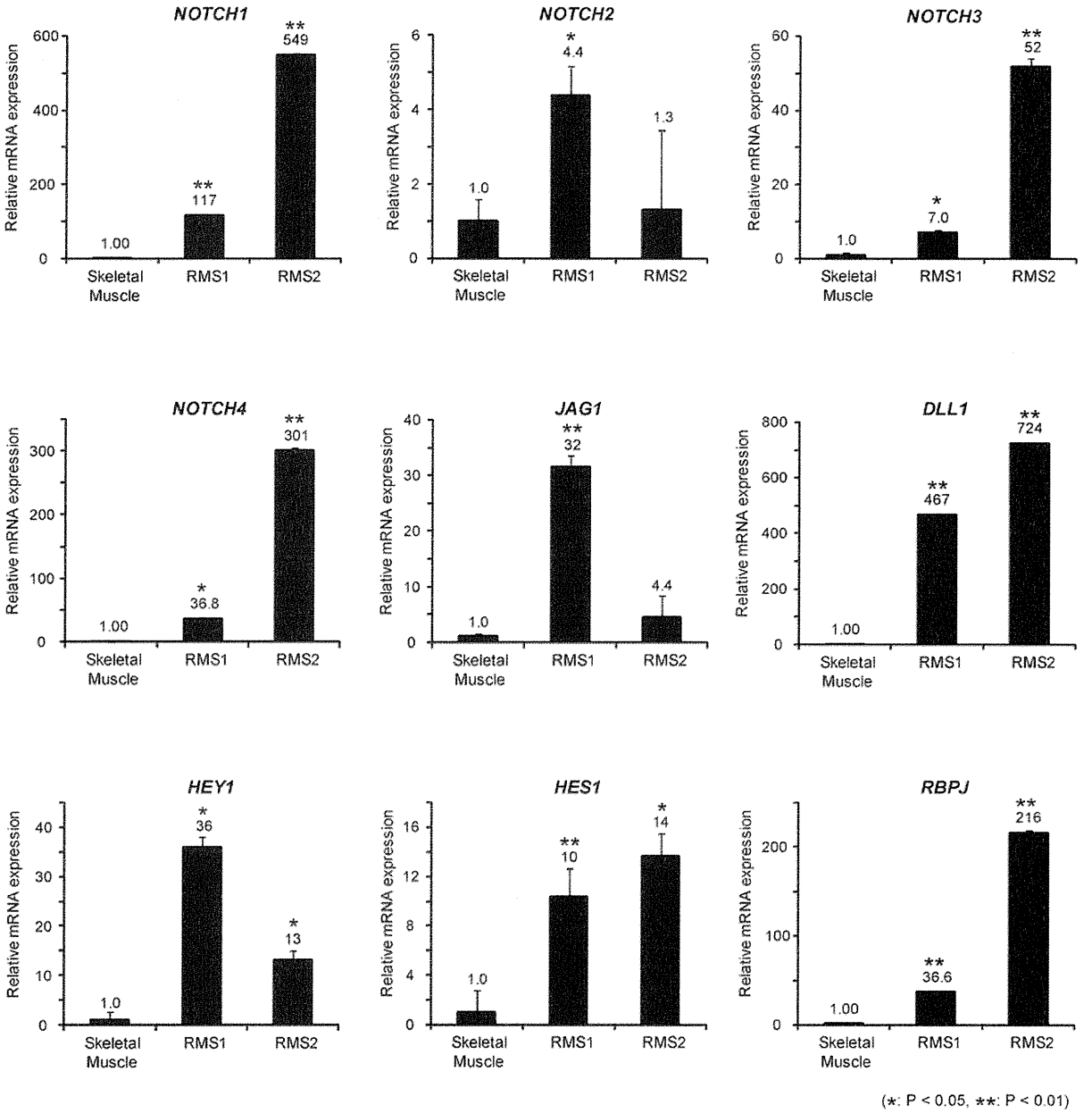

Figure 1. Notch pathway molecules are overexpressed in rhabdomyosarcoma cells. Notch pathway genes (receptors *NOTCH1-4*, ligands *JAG1* and *DLL1*, target genes *HES1* and *HEY1*, and transcription factor *RBPJ*) were assessed by real-time PCR in a normal human skeletal muscle specimen and 2 human RMS biopsy specimens. The Ct values of all RMS samples were normalized to those of *ACTB*. The values of the human RMS specimens were compared with those of the human skeletal muscle sample, which is defined as a relative expression of 1.0. Columns, mean values of 3 independent experiments; bar, SD. *$p<0.05$, **$p<0.01$.
doi:10.1371/journal.pone.0039268.g001

[38,39]. However, previous studies have shown that GSIs can kill breast cancer cells because of their nonspecific effect through their ability to inhibit the proteasome rather than blocking γ-secretase activity [25]. Additionally, GSIs proteolyze not only Notch receptor but also around 51 membrane proteins, including E-cadherin, VEGFR, and CXCL16 [40]. Furthermore, *HEY1* is involved in TGF-β pathway [41]. Thus, therapeutic strategies including treatment with GSIs or those targeting *HEY1* may affect other pathways. On the other hand, *RBPJ* acts only downstream of the Notch pathway, and nothing is known about its function in other pathways. Thus, we focused on the role of RBPJ to examine the bona fide function of the Notch pathway transcription factor in RMS tumorigenesis. The loss-of-function and gain-of-function of *RBPJ* indicated that *RBPJ* controled RMS cell growth *in vitro*. Although GSI treatment decreased the proliferation of RMS cells, knockdown of RBPJ did not decrease the proliferation in normal

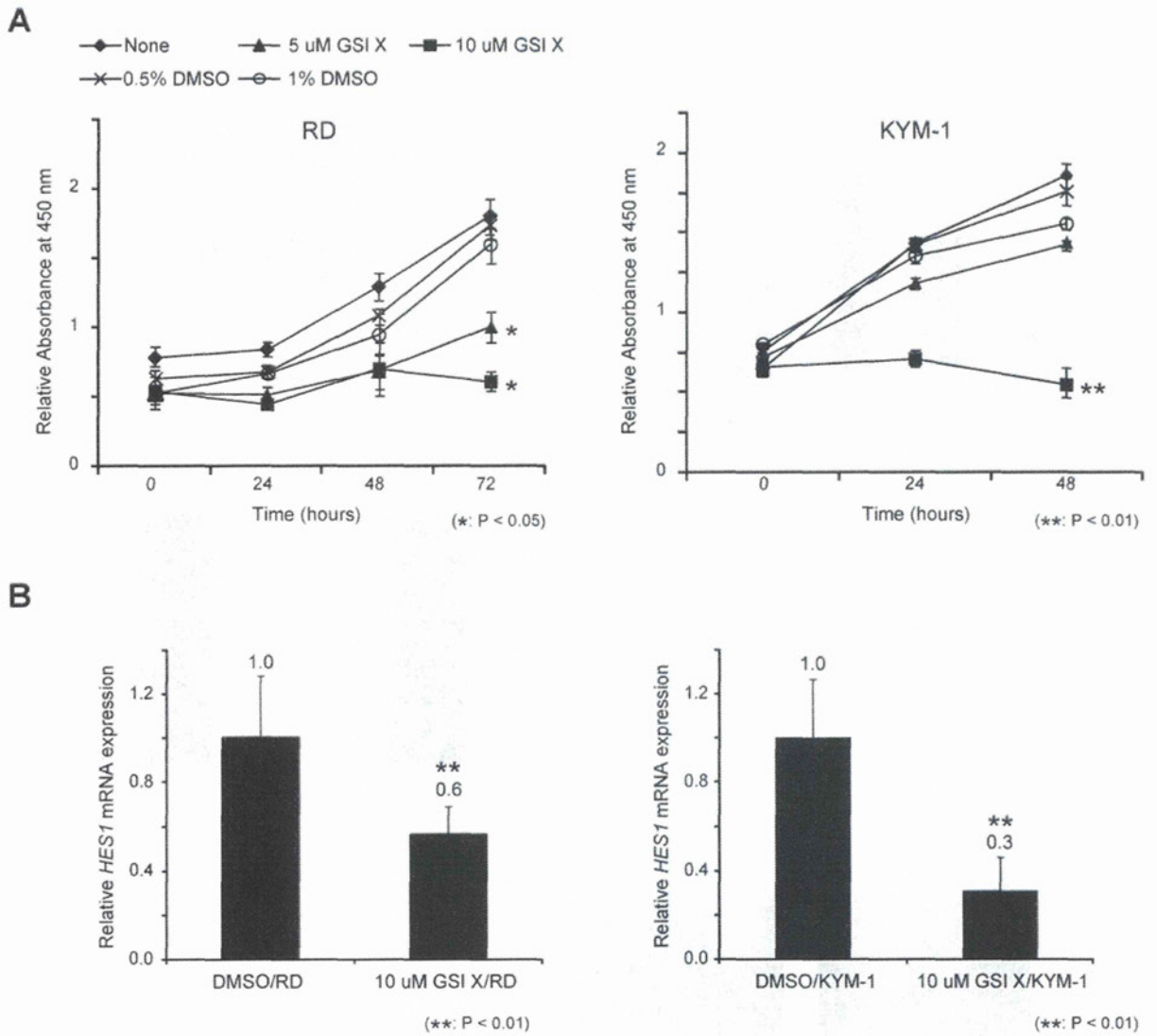

Figure 2. Effects of GSI X on the proliferation of rhabdomyosarcoma cells. A, Proliferation of RD and KYM-1 cells treated with GSI X or equal volume of DMSO vehicle were measured by WST-1 assay. **B**, Expression of *HES1* mRNA was assessed by real-time PCR in RD cells (left) and KYM-1 cells (right) treated with 10 μM of GSI X for 24 hours. Columns and lines, mean values of 3 independent experiments; bar, SD. $*p<0.05$, $**p<0.01$.

doi:10.1371/journal.pone.0039268.g002

culture condition (data not shown). These findings suggest that GSI inhibit Notch pathway more intensively than RBPJ knockdown or might affect not only Notch pathway but also other signaling pathways. On the other hand, knockdown of RBPJ prevented RMS proliferation in soft agar (3D culture) and *in vivo*. In addition, knockdown of *RBPJ* caused significantly improved the survival of mice. These findings suggest that transcription of RBPJ activated by Notch pathway is essential for RMS proliferation in physiological conditions. Although these three studies inhibit Notch signaling by inhibitor or knockdown of different genes, all studies provide independent support for the idea that Notch pathway plays essential roles in RMS progression. Furthermore, Notch pathway plays essential roles in many cancers [19,30,31,32]. Our results show that direct inhibition of *RBPJ* may offer a novel approach for inhibition of the Notch pathway not only in RMS but also in many cancers.

We showed that knockdown of *RBPJ* suppressed the expression of *Cyclin D*, *Cyclin E*, *E2F1*, and *SKP2*, whereas the expression of *p21* increased in *RBPJ* shRNA-transfected xenograft. SKP2, a subunit of the ubiquitin-ligase complex SCF^{SKP2}, is necessary for the degradation of p21 at the G1/S transition and during S phase in the cell cycle [42]. p21 inhibits CDK4-Cyclin D and thus suppresses the phosphorylation of RB and the sequestration of E2F1 and Cyclin E [43]. Therefore, our findings suggest that the inhibition of RBPJ prevents RMS growth *in vivo* by regulation of G1/S transition of the cell cycle.

Several studies have shown the relation between the Notch pathway and tumor-initiating cells (TICs) [44], and Sullivan *et*

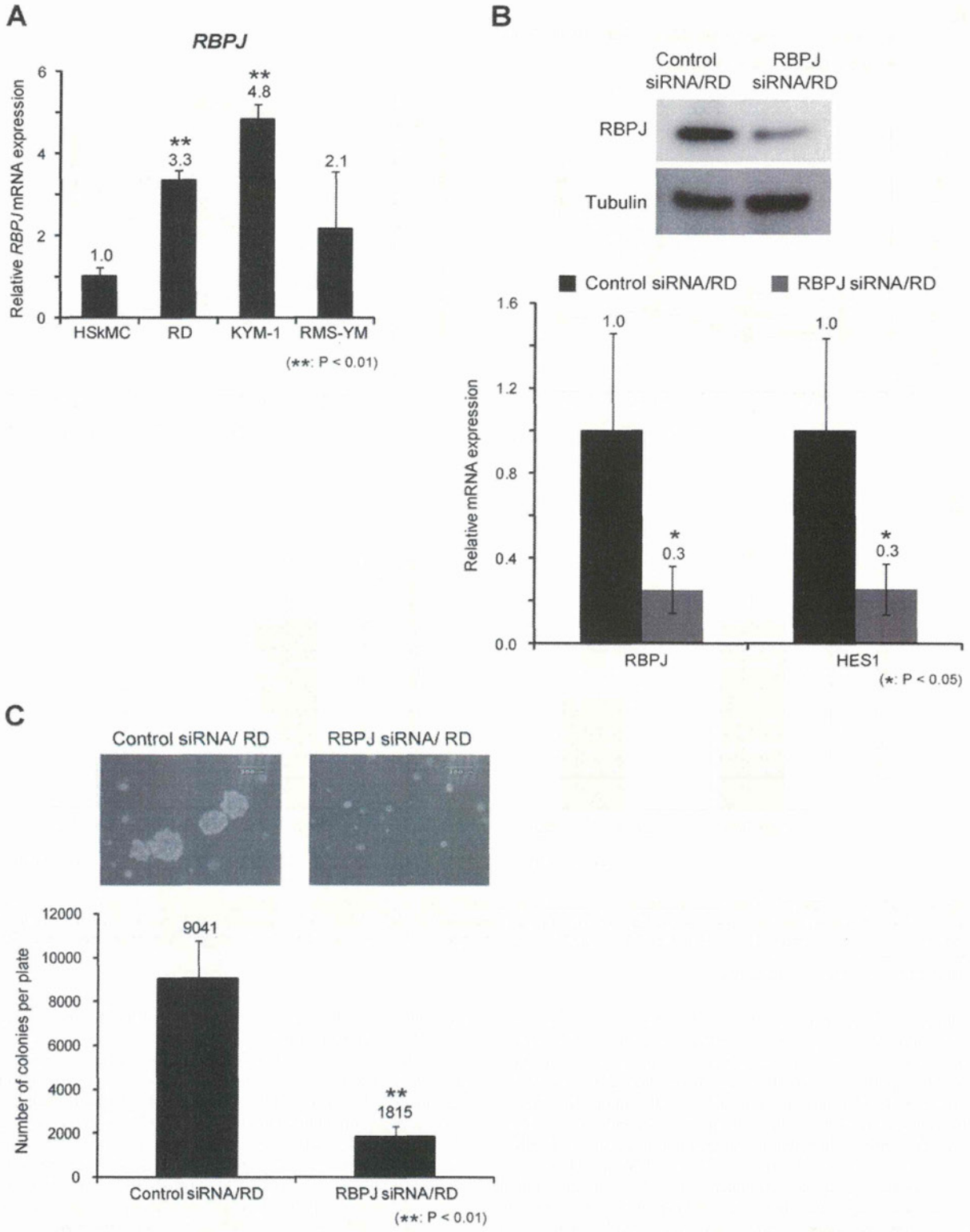

Figure 3. Knockdown of *RBPJ* suppresses anchorage-independent growth of rhabdomyosarcoma cells. A, The expression of *RBPJ* mRNA in RD cells was assessed by real-time PCR. The Ct values of all RMS cell lines were normalized to those of *ACTB*. The values of the RMS cell lines were compared with HSkMc cell, which is defined as a relative expression of 1.0. **B,** RBPJ protein levels in RD cells transfected with control and RBPJ siRNA

were examined by western blotting analysis (top). *RBPJ* and *HES1* mRNA in RD cells transfected with control and *RBPJ* siRNA were assessed by real-time PCR analysis. Ct values of *RBPJ* and *HES1* were normalized to *ACTB*. The values of the cells transfected with *RBPJ* siRNA were compared to those the RD cells transfected with control siRNA, which is defined as a relative expression of 1.0 (bottom). **C,** Anchorage-independent growth of RD cells transfected with control and *RBPJ* siRNA were evaluated by colony formation assay. After 3 weeks, each of the colonies were counted and photographed. Scale bar is 200 μM. Columns, mean values of 3 independent experiments; bar, SD. *$p<0.05$, **$p<0.01$.
doi:10.1371/journal.pone.0039268.g003

al. reported that aldehyde dehydrogenase (ALDH) activity selected for lung TICs is dependent on the Notch pathway [45]. Thus, we confirmed ALDH activity for the Notch pathway in RMS cell lines. However, no significant difference was observed in ALDH-positive population between *RBPJ* shRNA- and control shRNA-transfected RD cells (data not shown). Previously, we reported that the RMS cell lines included fibroblast growth factor receptor 3 (FGFR3)-positive TICs, which have high tumorigenic potential *in vivo* [46]. Hence, we examined the expression of FGFR3 in *RBPJ* shRNA- or control shRNA-transfected RD; however, no significant difference was observed in FGFR3-positive population in these cell lines (data not shown). These findings suggest that *RBPJ* does not have the roles in maintenance of ALDH or FGFR3-positive TICs in RMS cell lines. Recently, it has been reported that RMS cells contains a CD133-positive TICs [47,48]. Thus, further studies to explore that the relation between the Notch pathway and CD133-positive RMS TICs are needed to elucidate the pathogenesis of RMS.

Major advances have been made for understanding the interactions between the Notch pathway and other pathways during carcinogenesis [6,7]. Schreck *et al.* reported that the Notch target *HES1* directly modulated *GLI1*, transcription factor of the Hedgehog pathway, in glioblastoma cells [49]. Additionally, we showed that the Hedgehog pathway was activated in human RMS [23]. Targeting both the Notch pathway and the Hedgehog pathway simultaneously may be more effective in eliminating RMS cells.

In conclusion, we revealed that the Notch pathway is functionally activated in RMS. Our findings show that inhibition of *RBPJ* prevents the growth of RMS *in vitro* and *in vivo*. These novel findings improve the understanding of the pathogenesis of RMS and suggest that *RBPJ* may be an attractive therapeutic target for patients with RMS.

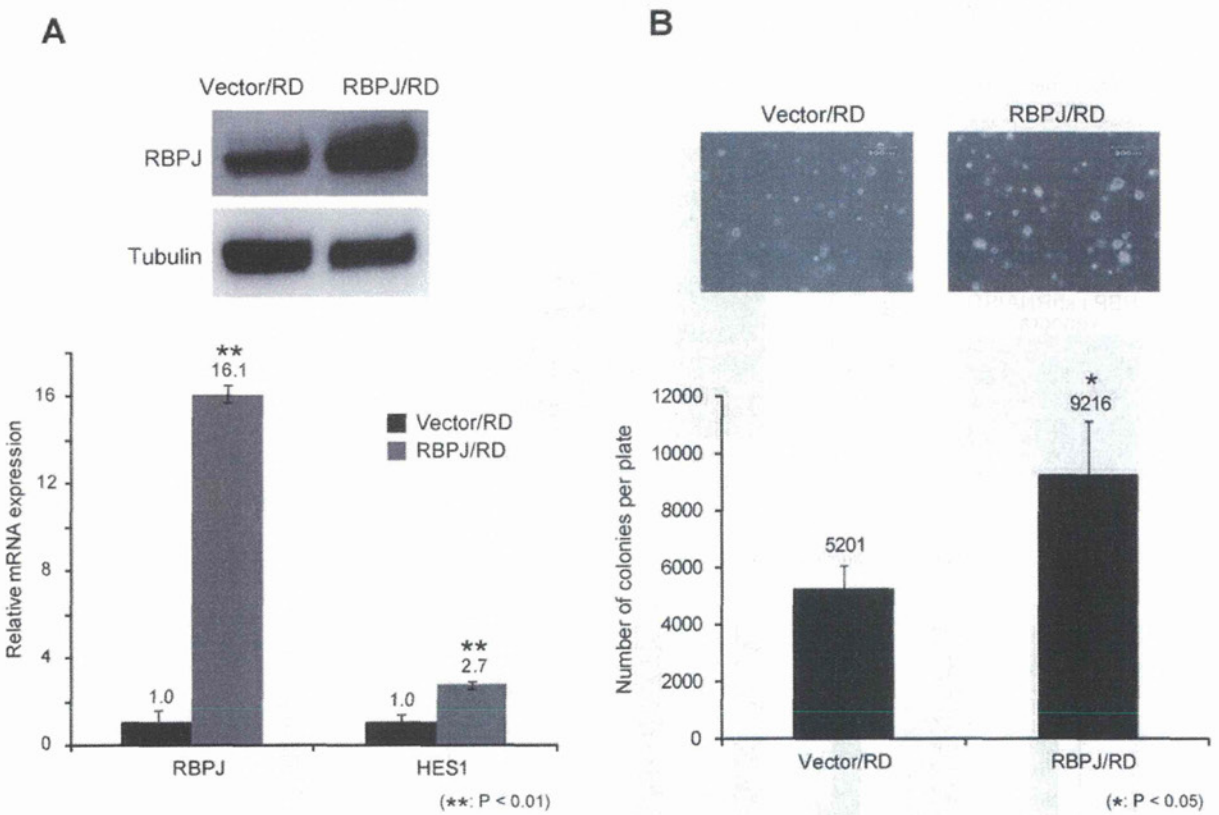

Figure 4. Overexpression of *RBPJ* promotes rhabdomyosarcoma cell growth. A, RBPJ protein levels in RD cells transfected with control vector and *RBPJ* overexpression vector were measured by Western blotting analysis (top). *RBPJ* and *HES1* mRNA in RD cells transfected with control vector and *RBPJ* overexpression vector were assessed by real-time PCR analysis. Ct values of *RBPJ* and *HES1* were normalized to *ACTB*. Comparison was made to the RD cells transfected control vector, which is defined as a relative expression of 1.0 (bottom). **B,** Anchorage-independent growth in RD cells transfected with control vector and *RBPJ* overexpression vector were evaluated by colony formation assay. Fourteen days later, the each colonies were counted and pictured. Scale bar is 200 μM. Columns, mean values of 3 independent experiments; bar, SD. *$p<0.05$, **$p<0.01$.
doi:10.1371/journal.pone.0039268.g004

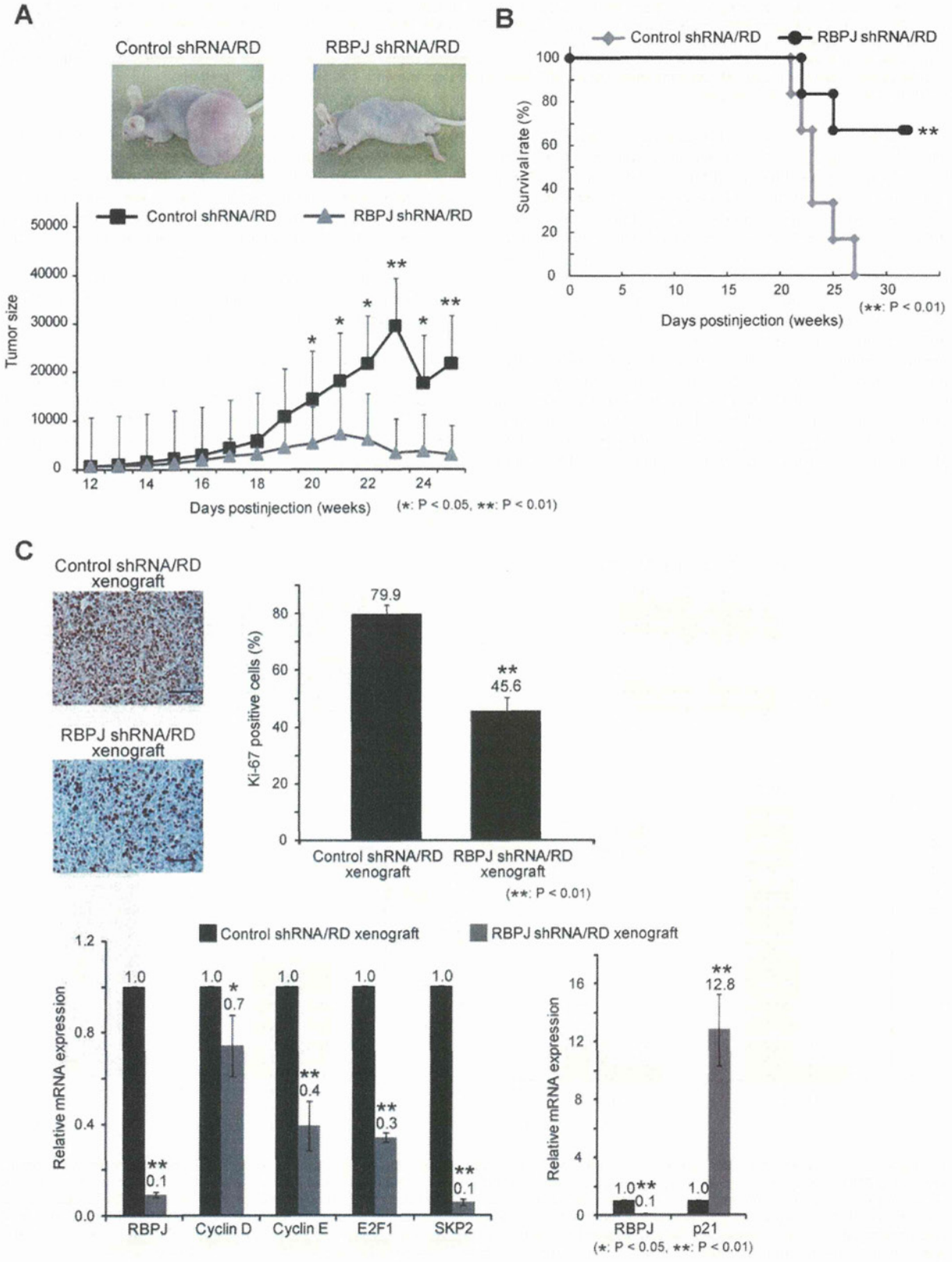
A
Control shRNA/RD
RBPJ shRNA/RD
Control shRNA/RD
RBPJ shRNA/RD
Tumor size
Days postinjection (weeks)
(*: P < 0.05, **: P < 0.01)
B
Control shRNA/RD
RBPJ shRNA/RD
Survival rate (%)
Days postinjection (weeks)
(**: P < 0.01)
C
Control shRNA/RD xenograft
RBPJ shRNA/RD xenograft
Ki-67 positive cells (%)
79.9
45.6
Control shRNA/RD xenograft
RBPJ shRNA/RD xenograft
(**: P < 0.01)
Control shRNA/RD xenograft
RBPJ shRNA/RD xenograft
Relative mRNA expression
RBPJ
Cyclin D
Cyclin E
E2F1
SKP2
Relative mRNA expression
RBPJ
p21
(*: P < 0.05, **: P < 0.01)

Figure 5. Knockdown of *RBPJ* inhibits the growth of rhabdomyosarcoma in nude mice. A, After transfection of control shRNA or *RBPJ* shRNA, 1×10^6 RD cells were subcutaneously inoculated in nude mice (n = 7). Tumor size was calculated weekly by using the formula $LW^2/2$ (with L and W representing the length and width of tumors). **B,** Survival rate of the mice injected with control shRNA- or *RBPJ* shRNA-transfected RD cells was assessed by Kaplan–Meier analysis. **C,** The number of Ki67-positive cells in control shRNA- or RBPJ shRNA-transfected xenograft were accessed by immnohistochemistry. Scale bar is 100 μm. Expression of Cell cycle-related genes (*CyclinD, CyclinE, E2F1, SKP2, p21*) were assessed by real-time PCR in control shRNA- or RBPJ shRNA-transfected xenograft. The Ct values of xenograft samples were normalized to those of *ACTB*. The values of the RBPJ shRNA-transfected xenograft was compared with those of the control shRNA sample, which is defined as a relative expression of 1.0. Columns, mean values of 3 independent experiments. Bar, SD. $*p<0.05$, $**p<0.01$.
doi:10.1371/journal.pone.0039268.g005

Supporting Information

Figure S1 Notch pathway molecules are overexpressed in rhabdomyosarcoma cell lines. Expression of Notch pathway genes (receptors *NOTCH1-4*, ligands *JAG1* and *DLL1*, target genes *HES1*, and *HEY1*) were assessed by real-time PCR in a human skeletal muscle cell line (HSkMC) and 3 human RMS cell lines. The Ct values of all RMS samples were normalized to those of *ACTB*. The values of the human RMS specimens were compared with those of the human skeletal muscle sample, which is defined as a relative expression of 1.0. Columns, mean values of 3 independent experiments. Bar, SD. $*p<0.05$, $**p<0.01$.
(TIF)

Figure S2 GSI XX prevents proliferation of rhabdomyosarcoma cells. RD and KYM-1 cells were treated with GSI XX or equal volume of DMSO vehicle. GSI XX treatment prevented the RMS proliferation.
(TIF)

Figure S3 GSI X treatment did not promote rhabdomyosarcoma cell apoptotic cell death. A, PARP and cleaved PARP protein levels in RD and KYM-1 cells were examine following 10 μM GSI X or equal volume of DMSO vehicle treatment. We used the PARP antibody which detect both full length PARP and cleaved PARP. Western blotting analysis revealed that GSI X treatment did not increase the expression of cleaved PARP. **B,** RD and KYM-1 cells were stained with Hoechst 33342 dye following 10 μM GSI X or equal volume of DMSO vehicle treatment. Apoptotic small body was not increased by GSI X treatment. Scale bar is 100 μm.
(TIF)

Acknowledgments

We are grateful to Hui Gao for the excellent technical assistance. We wish to thank the Joint-research laboratory of Kagoshima University Graduate School of Medical and Dental Sciences.

Author Contributions

Conceived and designed the experiments: TS HN S. Kitamoto S. Komiya. Performed the experiments: HN. Analyzed the data: YI SN SM. Contributed reagents/materials/analysis tools: MA MY NK SY. Wrote the paper: HN TS.

References

1. Wachtel M, Schafer BW (2010) Targets for cancer therapy in childhood sarcomas. Cancer Treat Rev 36: 318–327.
2. Rodeberg D, Paidas C (2006) Childhood rhabdomyosarcoma. Semin Pediatr Surg 15: 57–62.
3. Wachtel M, Schafer BW (2010) Targets for cancer therapy in childhood sarcomas. Cancer Treat Rev 36: 318–327.
4. Gupta AA, Anderson JR, Pappo AS, Spunt SL, Dasgupta R, et al. (2011) Patterns of chemotherapy-induced toxicities in younger children and adolescents with rhabdomyosarcoma: A Report From the Children's Oncology Group Soft Tissue Sarcoma Committee. Cancer 118: 1130–1137.
5. Perez EA, Kassira N, Cheung MC, Koniaris LG, Neville HL, et al. (2011) Rhabdomyosarcoma in Children: A SEER Population Based Study. J Surg Res 170: e243–e251.
6. Ranganathan P, Weaver KL, Capobianco AJ (2011) Notch signalling in solid tumours: a little bit of everything but not all the time. Nat Rev Cancer 11: 338–351.
7. Leong KG, Karsan A (2006) Recent insights into the role of Notch signaling in tumorigenesis. Blood 107: 2223–2233.
8. Fiuza UM, Arias AM (2007) Cell and molecular biology of Notch. J Endocrinol 194: 459–474.
9. Bray SJ (2006) Notch signalling: a simple pathway becomes complex. Nat Rev Mol Cell Biol 7: 678–689.
10. Gordon WR, Arnett KL, Blacklow SC (2008) The molecular logic of Notch signaling–a structural and biochemical perspective. J Cell Sci 121: 3109–3119.
11. Kopan R, Ilagan MX (2009) The canonical Notch signaling pathway: unfolding the activation mechanism. Cell 137: 216–233.
12. Allenspach EJ, Maillard I, Aster JC, Pear WS (2002) Notch signaling in cancer. Cancer Biol Ther 1: 466–476.
13. Radtke F, Raj K (2003) The role of Notch in tumorigenesis: oncogene or tumour suppressor? Nat Rev Cancer 3: 756–767.
14. Nickoloff BJ, Osborne BA, Miele L (2003) Notch signaling as a therapeutic target in cancer: a new approach to the development of cell fate modifying agents. Oncogene 22: 6598–6608.
15. Hsieh JJ, Henkel T, Salmon P, Robey E, Peterson MG, et al. (1996) Truncated mammalian Notch1 activates CBF1/RBPJk-repressed genes by a mechanism resembling that of Epstein-Barr virus EBNA2. Mol Cell Biol 16: 952–959.
16. Strobl LJ, Hofelmayr H, Stein C, Marschall G, Brielmeier M, et al. (1997) Both Epstein-Barr viral nuclear antigen 2 (EBNA2) and activated Notch1 transactivate genes by interacting with the cellular protein RBP-J kappa. Immunobiology 198: 299–306.
17. Aster JC, Blacklow SC, Pear WS (2010) Notch signalling in T-cell lymphoblastic leukaemia/lymphoma and other haematological malignancies. J Pathol 223: 262–273.
18. Sivasankaran B, Degen M, Ghaffari A, Hegi ME, Hamou MF, et al. (2009) Tenascin-C is a novel RBPJkappa-induced target gene for Notch signaling in gliomas. Cancer Res 69: 458–465.
19. Tanaka M, Setoguchi T, Hirotsu M, Gao H, Sasaki H, et al. (2009) Inhibition of Notch pathway prevents osteosarcoma growth by cell cycle regulation. Br J Cancer 100: 1957–1965.
20. Matsunoshita Y, Ijiri K, Ishidou Y, Nagano S, Yamamoto T, et al. (2011) Suppression of osteosarcoma cell invasion by chemotherapy is mediated by urokinase plasminogen activator activity via up-regulation of EGR1. PLoS One 6: e16234.
21. Kunigou O, Nagao H, Kawabata N, Ishidou Y, Nagano S, et al. (2011) Role of GOLPH3 and GOLPH3L in the proliferation of human rhabdomyosarcoma. Oncol Rep 26: 1337–1342.
22. Nagao H, Ijiri K, Hirotsu M, Ishidou Y, Yamamoto T, et al. (2011) Role of GLI2 in the growth of human osteosarcoma. J Pathol 224: 169–179.
23. Kawabata N, Ijiri K, Ishidou Y, Yamamoto T, Nagao H, et al. (2011) Pharmacological inhibition of the Hedgehog pathway prevents human rhabdomyosarcoma cell growth. Int J Oncol 39: 899–906.
24. Sasaki H, Setoguchi T, Matsunoshita Y, Gao H, Hirotsu M, et al. (2010) The knock-down of overexpressed EZH2 and BMI-1 does not prevent osteosarcoma growth. Oncol Rep 23: 677–684.
25. Han J, Ma I, Hendzel MJ, Allalunis-Turner J (2009) The cytotoxicity of gamma-secretase inhibitor I to breast cancer cells is mediated by proteasome inhibition, not by gamma-secretase inhibition. Breast Cancer Res 11: R57.
26. Ni CY, Murphy MP, Golde TE, Carpenter G (2001) gamma -Secretase cleavage and nuclear localization of ErbB-4 receptor tyrosine kinase. Science 294: 2179–2181.
27. Marambaud P, Shioi J, Serban G, Georgakopoulos A, Sarner S, et al. (2002) A presenilin-1/gamma-secretase cleavage releases the E-cadherin intracellular domain and regulates disassembly of adherens junctions. Embo J 21: 1948–1956.
28. Esler WP, Kimberly WT, Ostaszewski BL, Diehl TS, Moore CL, et al. (2000) Transition-state analogue inhibitors of gamma-secretase bind directly to presenilin-1. Nat Cell Biol 2: 428–434.
29. Artavanis-Tsakonas S, Rand MD, Lake RJ (1999) Notch signaling: cell fate control and signal integration in development. Science 284: 770–776.

30. Mullendore ME, Koorstra JB, Li YM, Offerhaus GJ, Fan X, et al. (2009) Ligand-dependent Notch signaling is involved in tumor initiation and tumor maintenance in pancreatic cancer. Clin Cancer Res 15: 2291–2301.
31. Stylianou S, Clarke RB, Brennan K (2006) Aberrant activation of notch signaling in human breast cancer. Cancer Res 66: 1517–1525.
32. Serafin V, Persano L, Moserle L, Esposito G, Ghisi M, et al. (2011) Notch3 signalling promotes tumour growth in colorectal cancer. J Pathol 224: 448–460.
33. Kuroda K, Tani S, Tamura K, Minoguchi S, Kurooka H, et al. (1999) Delta-induced Notch signaling mediated by RBP-J inhibits MyoD expression and myogenesis. J Biol Chem 274: 7238–7244.
34. Hirsinger E, Malapert P, Dubrulle J, Delfini MC, Duprez D, et al. (2001) Notch signalling acts in postmitotic avian myogenic cells to control MyoD activation. Development 128: 107–116.
35. Roma J, Masia A, Reventos J, Sanchez de Toledo J, Gallego S (2011) Notch pathway inhibition significantly reduces rhabdomyosarcoma invasiveness and mobility in vitro. Clin Cancer Res 17: 505–513.
36. Belyea BC, Naini S, Bentley RC, Linardic CM (2011) Inhibition of the Notch-Hey1 Axis Blocks Embryonal Rhabdomyosarcoma Tumorigenesis. Clin Cancer Res 17: 7324–7336.
37. Siemers ER, Quinn JF, Kaye J, Farlow MR, Porsteinsson A, et al. (2006) Effects of a gamma-secretase inhibitor in a randomized study of patients with Alzheimer disease. Neurology 66: 602–604.
38. van Es JH, van Gijn ME, Riccio O, van den Born M, Vooijs M, et al. (2005) Notch/gamma-secretase inhibition turns proliferative cells in intestinal crypts and adenomas into goblet cells. Nature 435: 959–963.
39. Tohda S, Sato T, Kogoshi H, Fu L, Sakano S, et al. (2006) Establishment of a novel B-cell lymphoma cell line with suppressed growth by gamma-secretase inhibitors. Leuk Res 30: 1385–1390.
40. Beel AJ, Sanders CR (2008) Substrate specificity of gamma-secretase and other intramembrane proteases. Cell Mol Life Sci 65: 1311–1334.
41. Zavadil J, Cermak L, Soto-Nieves N, Bottinger EP (2004) Integration of TGF-beta/Smad and Jagged1/Notch signalling in epithelial-to-mesenchymal transition. Embo J 23: 1155–1165.
42. Sarmento LM, Huang H, Limon A, Gordon W, Fernandes J, et al. (2005) Notch1 modulates timing of G1-S progression by inducing SKP2 transcription and p27 Kip1 degradation. J Exp Med 202: 157–168.
43. Abbas T, Dutta A (2009) p21 in cancer: intricate networks and multiple activities. Nat Rev Cancer 9: 400–414.
44. Pannuti A, Foreman K, Rizzo P, Osipo C, Golde T, et al. (2010) Targeting Notch to target cancer stem cells. Clin Cancer Res 16: 3141–3152.
45. Sullivan JP, Spinola M, Dodge M, Raso MG, Behrens C, et al. (2010) Aldehyde dehydrogenase activity selects for lung adenocarcinoma stem cells dependent on notch signaling. Cancer Res 70: 9937–9948.
46. Hirotsu M, Setoguchi T, Matsunoshita Y, Sasaki H, Nagao H, et al. (2009) Tumour formation by single fibroblast growth factor receptor 3-positive rhabdomyosarcoma-initiating cells. Br J Cancer 101: 2030–2037.
47. Sana J, Zambo I, Skoda J, Neradil J, Chlapek P, et al. (2011) CD133 expression and identification of CD133/nestin positive cells in rhabdomyosarcomas and rhabdomyosarcoma cell lines. Anal Cell Pathol 34: 1–16.
48. Walter D, Satheesha S, Albrecht P, Bornhauser BC, D'Alessandro V, et al. (2011) CD133 positive embryonal rhabdomyosarcoma stem-like cell population is enriched in rhabdospheres. PLoS One 6: e19506.
49. Schreck KC, Taylor P, Marchionni L, Gopalakrishnan V, Bar EE, et al. (2010) The Notch target Hes1 directly modulates Gli1 expression and Hedgehog signaling: a potential mechanism of therapeutic resistance. Clin Cancer Res 16: 6060–6070.

Lung Cancer 78 (2012) 144–147

Contents lists available at SciVerse ScienceDirect

Lung Cancer

journal homepage: www.elsevier.com/locate/lungcan

EGFR mutations and human papillomavirus in lung cancer

Takuya Kato[a], Chihaya Koriyama[a,*], Noureen Khan[a], Takuya Samukawa[b], Masakazu Yanagi[c], Tsutomu Hamada[b], Naoya Yokomakura[c], Takeshi Otsuka[c], Hiromasa Inoue[b], Masami Sato[d], Shoji Natsugoe[c], Suminori Akiba[a]

[a] Department of Epidemiology and Preventive Medicine, Graduate School of Medical and Dental Sciences, Kagoshima University, 8-35-1 Sakuragaoka, Kagoshima 890-8544, Japan
[b] Department of Pulmonary Medicine, Graduate School of Medical and Dental Sciences, Kagoshima University, 8-35-1 Sakuragaoka, Kagoshima 890-8544, Japan
[c] Department of Surgical Oncology and Digestive Surgery, Graduate School of Medical and Dental Sciences, Kagoshima University, 8-35-1 Sakuragaoka, Kagoshima 890-8544, Japan
[d] Department of General Thoracic Surgery, Graduate School of Medical and Dental Sciences, Kagoshima University, 8-35-1 Sakuragaoka, Kagoshima 890-8544, Japan

ARTICLE INFO

Article history:
Received 20 April 2012
Received in revised form 6 August 2012
Accepted 18 August 2012

Keywords:
Epidermal growth factor receptor
Mutation
Human papillomavirus
Adenocarcinoma
Gefitinib

ABSTRACT

Our previous study reported a frequent detection of human papillomavirus (HPV) genome in primary lung adenocarcinomas of the recurrent patients who were responsive to epidermal growth factor receptor (EGFR)-tyrosine kinase inhibitor, suggesting that HPV presence in lung cancer may be related to a genetic background related to EGFR mutations. The present study examined the association between the HPV presence and mutations in exons 19 and 21 of EGFR gene in Japanese lung cancer patients. Thirteen (31%) out of 42 cases had EGFR mutations. Although these mutations were tended to be observed in females, non-smokers, or adenocarcinomas, there was no statistically significant associations. HPV DNA was found in 7/42 (17%) lung tumors. The frequency of HPV presence did not differ in histological types. The presence of HPV DNA was significantly related to EGFR mutations ($P = 0.021$), especially in adenocarcinomas of the lung ($P = 0.014$). HPV-positive lung tumors accounted for 38% and 7% of those with and without EGFR mutations, respectively. Our results suggest that EGFR mutations are associated with HPV presence in Japanese patients with lung cancer.

1. Introduction

Human papillomavirus (HPV) is a well-established risk factor of cervical cancer [1]. HPV types 16 and 18 are classified as carcinogenic to humans (Group 1) by International Agency for Research on Cancer [2], and these HPV types were also detected in a part of lung cancer [3]. In spite of many studies reporting the HPV presence, its role in lung carcinogenesis is still unclear. Although HPV-16 integration in host genome has been reported in the most of HPV-16-positive lung squamous cell carcinomas (SQCs) [4], its low viral load makes it difficult to determine the etiological significance.

A Taiwanese study reported a significant association between HPV-16/18 and lung adenocarcinomas (ACs) among nonsmoking female patients [5]. We also reported a higher prevalence of high-risk HPV in ACs (30%, 9/30) than that of SQCs (7%, 2/27) [6]. Furthermore, high-risk HPV genome was more frequently observed in lung ACs with response to gefitinib (75%, 6/8) than that of those without response to the treatment (0%, 0/12) [6].

Clinical responsiveness to gefitinib is associated with somatic mutations in the tyrosine kinase domain of the epidermal growth factor receptor (EGFR) gene [7,8], which are most frequently observed in lung ACs of non-smoking women in far-East Asian countries [9]. It is worth noting that these clinicopathological features, non-smoking female lung ACs, are similar to that observed in the Taiwanese study [5].

In the present study, we investigated the association between EGFR mutations and the presence of HPV DNA in Japanese lung cancer. Furthermore, viral load and physical status of high-risk HPV-16 were examined.

2. Materials and methods

2.1. Clinical specimens

The present study examined a total of 42 paraffin-embedded tissue samples of lung cancer cases, including 26 ACs, 12 SQCs and 4 other histological types, diagnosed at Kagoshima University Hospital during the period from December 2007 to December 2008. Institutional Review Boards of Kagoshima University Hospital, Japan, approved the present study.

* Corresponding author. Tel.: +81 99 275 5298; fax: +81 99 275 5299.
E-mail address: fiy@m.kufm.kagoshima-u.ac.jp (C. Koriyama).

0169-5002/$ – see front matter © 2012 Elsevier Ireland Ltd. All rights reserved.
http://dx.doi.org/10.1016/j.lungcan.2012.08.011

Table 1
Clinicopathological features of lung tumors by the presence of EGFR mutation and HPV genome.

	Total	EGFR		HPV	
		Mutated	*P*-Value[a]	Positive	*P*-Value[a]
Total	42 (100%)	13 (31%)		7 (17%)	
Age			0.505		1.000
<70	17 (100%)	4 (24%)		3 (18%)	
≥70	25 (100%)	9 (36%)		4 (16%)	
Sex			0.082		0.197
Female	14 (100%)	7 (50%)		4 (29%)	
Male	28 (100%)	6 (21%)		3 (11%)	
Smoking			0.181		1.000
Never	21 (100%)	9 (43%)		4 (19%)	
Ever	21 (100%)	4 (19%)		3 (14%)	
Histology			0.471		0.839
Adenocarcinoma	26 (100%)	10 (38%)		4 (15%)	
Squamous cell ca.	12 (100%)	2 (17%)		2 (17%)	
Others[b]	4 (100%)	1 (25%)		1 (25%)	
Clinical stage			0.739		1.000
I	27 (100%)	9 (33%)		5 (19%)	
II–IV	15 (100%)	4 (27%)		2 (13%)	
Tumor size			0.043		1.000
≤3 cm	21 (100%)	10 (48%)		4 (19%)	
>3 cm	21 (100%)	3 (14%)		3 (14%)	
Histological differentiation[c]			0.870		0.809
Well	27 (100%)	10 (37%)		5 (19%)	
Moderate	6 (100%)	2 (33%)		1 (17%)	
Poor	5 (100%)	1 (20%)		0 (0%)	
Lymph node metastasis			0.127		0.160
No	30 (100%)	12 (40%)		7 (23%)	
Yes	11 (100%)	1 (9%)		0 (0%)	
Unknown	1 (100%)	0 (0%)		0 (0%)	
Distant metastasis			0.529		0.309
No	40 (100%)	12 (30%)		6 (15%)	
Yes	2 (100%)	1 (50%)		1 (50%)	

[a] *P*-Values were obtained by Fisher's exact test.
[b] Other histology: 2 carcinoids and 2 adenosquamous carcinomas.
[c] Histological differentiation was not available.

2.2. HPV detection, typing and physical status

The HPV genome was detected by PCR with broad-spectrum SPF10-biotinylated primers [10]. HPV typing was performed using the INNO-LiPA HPV Genotyping CE test (Innogenetics, Ghent, Belgium). To determine the presence and physical status, as well as estimate the viral load of HPV-16, the quantitative real-time PCR was performed using 2× QuantiTect SYBR Green PCR kit (QIAGEN, Hilden, Germany). The physical status of HPV-16 was determined by the method proposed by Peitsaro et al. [11], assuming that: (i) preferential disruption of E2 causes absence of E2 gene sequence in the PCR product following integration and (ii) the copy number of both E2 and E6 genes should be equal when viral DNA presents in episomal form.

2.3. Examination of EGFR mutations

The sensitivity of lung ACs to gefitinib is associated with EGFR mutations, which include (i) exon 19 deletion of amino acids 747–750, accounting for 45% of mutations and (ii) exon 21 mutation resulting in L858R substitution, accounting for 40–45% of mutations [12]. Mutations in exons 19 and 21 were detected on the basis of the method using PCR proposed by Sugio et al. [13]. The results of PCR assay for exon 21 L858R was confirmed using a base sequence analysis.

3. Results

Among 42 lung tumors, 13 cases (31%) had mutations in either exon 19 or 21 of the EGFR gene (Table 1). Exon 19 deletion and exon 21 L858R were detected in 7 (54%) and 6 (46%) out of 13 mutations, respectively. These mutations were mutually exclusive. The frequency of the mutations was significantly higher in smaller tumors (Table 1, $P=0.043$).

HPV DNA was detected in 7/42 (17%) lung tumors (Table 1). HPV-16 was the most frequently detected type ($n=5$). High-risk HPV-58 was detected in the remaining two cases. The geometric mean of HPV-16 viral load was 0.003 per cell (shown in a supplement) and was much lower than that observed in cervical cancer (geometric mean of HPV-16 = 333 copies per cell; unpublished data). None of the clinicopathological factors was related to the HPV presence (Table 1).

The presence of HPV DNA was significantly related to EGFR mutations (Table 2, $P=0.021$). This association was significant in ACs of the lung ($P=0.014$). All HPV-16-positive ACs ($n=3$) were considered to have HPV integration into the host genome, and all of them had exon 19 deletion (shown in a supplement).

4. Discussion

The present study showed a significant association between high-risk HPV detection and EGFR mutations in Japanese lung cancer cases ($P=0.021$). Similar results were described in a Taiwanese study [14]. On the other hand, EGFR mutations were quite rare in cervical cancer [15], and the EGFR mutations were not related to HPV presence in SQCs of the tongue and tonsil [16]. These findings suggest that the association between EGFR mutations and HPV presence is restricted to lung cancer.

HPV-16 integration was observed in tumors with exon 19 deletion mutant. Although both exon 19 deletion and exon 21 L858R increase phosphorylation of EGFR leading to cell survival promotion through AKT pathway [17], the response rate to gefitinib was